Additional Thesis Report

Numerical Investigation on the Effect of Scour Formation & Scour Protection on the Stiffness & Lateral Capacity of Monopiles

Student
Georgios Chortis (4578813)

Supervisors
Dr. Amin Askarinejad
Dr. Luke Prendergast

TU Delft Delft University of Technology

July 2018

Preface

The aim of this additional thesis is the investigation of the effect of the scour formation and protection in the stiffness and the lateral capacity of an offshore monopile. The investigation was conducted in the finite element code PLAXIS 3D. Working in this software with a sophisticated constitutive model was really exciting for me, as it offered me a great deal of skills, knowledge and motivation to learn more for the numerical modelling.

I would like to thank my supervisor, Dr. Amin Askarinejad, for granting me the chance to work in such an exciting project and for an excellent co-operation in the whole duration of the project. He offered me a lot of advice and a professional aspect in our weekly meetings. Of course I would also like to thank Dr. Luke Prendergast who kindly accepted the invitation to be part of the committee that assess this project. Last but not least, I owe many thanks to Dr. Ronald Brinkgreve, with whom I had an enlightening discussion about using the hypoplasticity model in PLAXIS analyses.

I would also like to show my appreciation to my colleagues, Antonis, Konstantinos and Vassilis. More specifically, Antonis is like an academic mentor to me, as he introduced me to the TU Delft, Konstantinos' judgement proved to be a valuable asset in providing a high quality work and Vassilis' critical thinking and eye for the detail helped me to produce a valid, scientific result. In many occasions we have all discussed about my work and I was lucky enough to be granted with their scientific judgement and point of view. A lot of special thanks are also given to Eleni, that supported me during this project, especially when difficulties have arisen, contributing to the completion of this project.

Many thanks are also necessary to be granted to my friends Nikiforos, Dimitris, Tzori and Dionysia who have stood to me during the whole period of studying in TU Delft. My little experience as a student has showed me that working in a friendly environment with support and trust allows for high quality work, which I have tried my best to produce.

I would also like to thank my brother, who was the first to inspire me to follow the engineering path from a rather young age, and my parents as they gave me the opportunity to study in TU Delft along with the means to hopefully become an accomplished engineer.

Giorgos Chortis

July 2018

Abstract

Wind turbines are nowadays the main means for producing renewable energy in Northern and Western Europe, and therefore research is conducted to secure their efficiency. One of the critical aspects of the windfarms is the foundation type, as it can define the functionality and the cost of each turbine. Monopiles have prevailed as the most efficient foundation, since 75% of the existing wind farms are founded in this way. However, despite their dominance, there are still mechanisms that affect their stability during their lifetime. Scour formation, which is the erosion of the soil around a monopile, is a crucial one that is the topic of this project. More specifically, the effect of the scour formation (both depth and type) in the stiffness and the lateral capacity in sandy soils has been investigated, followed by analyses about the efficiency of the scour protection layers. The methodology that was followed included numerical simulations, which have been performed in the finite element code of PLAXIS 3D. More specifically, 26 simulations have been conducted, in which the vertical load, the scour depth and type and the scour protection length were the parameters that have been investigated. The conclusions drawn could be divided into four categories, the vertical load, the scour depth and type and the scour formation effect in the stiffness and the lateral capacity. It was shown that the increase in the vertical load had a positive influence in the lateral capacity of the soil-monopile system. However, it could be characterized negligible, as the lateral capacity increase was less than 5%. In the next set of results, the scour depth impact in the stiffness and lateral capacity of the soil was investigated. It was observed that for the same type of scouring, the increase of the depth of the scour hole significantly reduced the soil resistance. It is noted though that scour up to 1.0D could be managed except for the global scour case. On the other hand, for larger depths the situation was becoming more critical and in depth of about 2.0D, the loss of the capacity was too great leading to a no-return state, for all scouring types. Then, the type of scouring impact was investigated, as local scour (narrow and wide) or global can occur. It was shown that the narrow type of scour was the most favorable case, which could approach the no scour case for small scour depth, while the global scour case was the most critical, as even in small scour depths could lead to dramatic reduction of the capacity. The main point is that the narrow case and the wide one can be manageable in depths up to 1.5D under certain conditions, while the global type seems to become a no-return case for much smaller erosion depths. The last part included the scour protection effect which was similar to the vertical load effect, as it had a positive influence in the lateral capacity of the soil-monopile system, but in a range of 5 to 15%. Therefore, it could be ignored in the design phase, unless a thicker protection layer is used. The graphs of the evolution of soil pressures and pile deflection clearly indicated that the monopile presents a rigid response, as the pile was rotated in all cases from a certain rotation point. The rigid behavior of the pile states that the API method is outdated as it is based on slender piles and it cannot capture the rotation point and the distribution of soil pressures that occur due to the rigidity of the monopile. The final output of this current report is a design recommendation, depicted in two normalized charts that correlate load and stiffness at failure displacements with the scour depth and type.

Table of Contents

List of Figures

List of Tables

Chapter 1

Introduction

The offshore wind industry has developed rapidly in the past years, as this sector offers a viable and eco-friendly alternative for supplying the world with part of the demanded energy. Western and Northern Europe now depend on windfarms to a certain extent for covering their energy needs. This new trend has led to a lot of research, focused on key aspects such as the foundation of the wind turbines, in order to secure their efficiency and sustainability. The monopiles have prevailed as the most efficient foundation, since they have been used to found over 75% of the existing wind farms (Doherty & Gavin, 2012). However, despite their dominance, there are certain mechanisms, such as scour formation, that affect the stability and functionality of the monopiles during their lifetime that needs to be investigated. American Petroleum Institute (API) method and regulations have been the base for the design of most offshore projects. However, their application in monopiles could not been characterized as efficient, since in-situ measurements were in disagreement with the expected ones from the design phase. In certain cases, the embedded part of the monopiles was prolonged beforehand to compensate for the unrealistic soil response provided by the API, increasing though the total cost of the projects. As a result, research is now focused on providing new design methods that will better capture the behavior of the monopile-system, allowing for efficient and accurate design. However, despite the findings that have occurred and the consequent methods proposed, there is still a gap in the literature review regarding the effect of the scour formation but also scour protection measures in the stiffness and the lateral capacity of the monopiles.

1.1 Scour Phenomenon

1.1.1 Scouring Process

Scour is defined as the erosion of the soil in the surrounding area of an object (such as a monopile) due to water flow caused by waves and mainly currents, creating a hole. It can be distinguished in two categories, the local scour and the global scour. In case of local scour, the hole that has been formed is limited in a small area around the pile. Global scour on the other hand, implies an erosion of the soil in a much larger area, deepening the seabed around the structure.

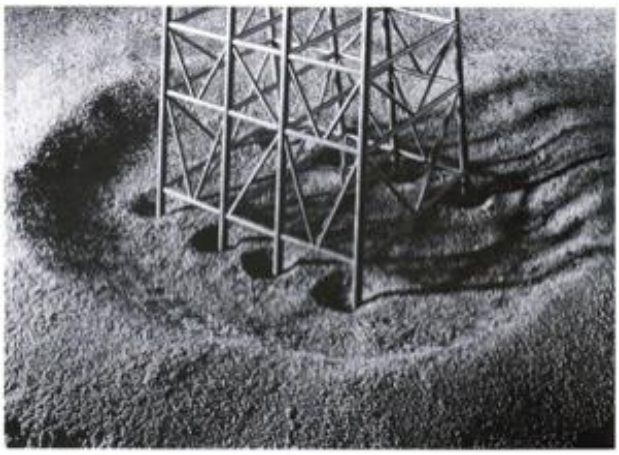

Figure 1.1 Local scour is observed in the hole that has been formed in each pile, while the global scour can be observed around the whole pile structure. Whitehouse, 1997

In general, if a single pile exists, local scour is formed, while in cases of large wind farms or extreme currents, global scour can occur. The main difference between the two types of scour lies in the perimeter of the hole and not in the depth which seems to be slightly larger in the local scour holes. In Figure 1.1 the distinction between local and global scour can be observed, as two different types of scour holes appear, one developed around each pile (local) and one larger developed in the whole area around the offshore structure (global).

The conducted research in the aforementioned topic is focused on the scour effect around a single typical monopile. It is common to examine both the cases of local and global scour formation. More specifically, in Figure 1.2, three types of scouring are presented, that are the most common cases investigated in the literature (Hjorth, 1975; L. C. Reese et al., 1989; B. Mutlu Sumer et al., 1992; Whitehouse, 1997; Hoffmans & Verheij, 1997; Kishore et al., 2009; Whitehouse et al., 2011; Y. E. Mostafa, 2012; Petersen et al., 2015; Qi et al., 2016). The first two cases, the wide and the narrow one, are characterized as the local scour type while the global scour formation cannot be distinguished in any other categories. In general, wide and narrow type scour formations are most frequent, as they may be caused by moderate waves and currents. The cyclic loading induced by the functionality of the wind turbine may have also an effect but negligible compared to the aforementioned actions (Whitehouse, 1997; Whitehouse et al., 2011). On the other hand, as already mentioned, global type of scour around a single monopile implies prevailing extreme currents in the foundation area, which are not often the case in a typical windfarm. However, the researchers are interested in the effect of both local and global scouring in the soil-monopile system response.

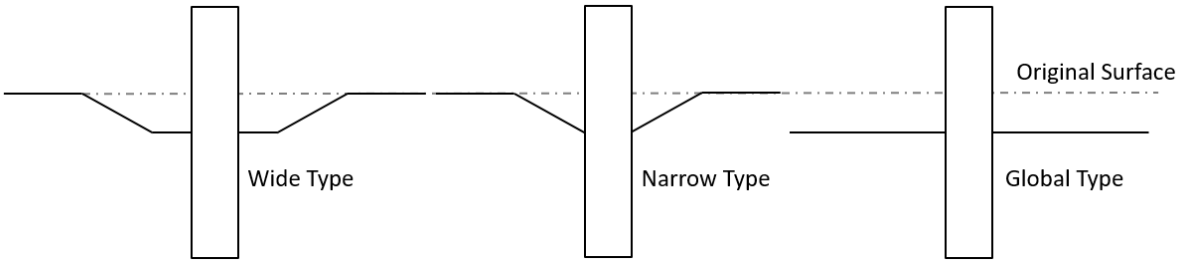

Figure 1.2 Different types of scour holes that may be formed around a typical monopile.

The scour depth is usually larger in the cases of local holes instead of soil erosion over a larger area. According to Kuo & Achmus, 2008 from the Leibniz University of Hannover, the researchers that have investigated the scour effect (such as Whitehouse, 2006 & Yasser E. Mostafa, 2012) have suggested in the design guideline of the OWEC that the scour depth that is estimated to be formed in a monopile is about 1.3 to 2.5 times the pile diameter. However, according to the same source during the design of a project, a less conservative value is adopted, as the scour factor is usually between 1.0 to 1.5 times the diameter.

1.1.2 Scour Protection Methods

The formation of a scour hole around a monopile can lead to a significant problem to the stability of the pile, which can even lead to failure of the monopile. However, the most common problem caused by the scour phenomenon is about the serviceability limits. More specifically, the developed displacements that are induced by the scour are usually not excessive, that imply failure, but large enough to not allow the proper function of the wind turbine, that is held by the pile. As a result, scour protection methods have been developed in cases where the currents and the waves are strong enough to erode the soil. Of course, scour protection is a preventive measure against scour but in many cases, the scour proved to be larger than expected due to lack of understanding of every aspect of the problem. As a result, mitigation measures have also been introduced in certain projects to deal with the scour hole that have been formed. Therefore, two different cases will be examined, one about the prevention (or limitation) of the scour and one about the mitigation of the scour.

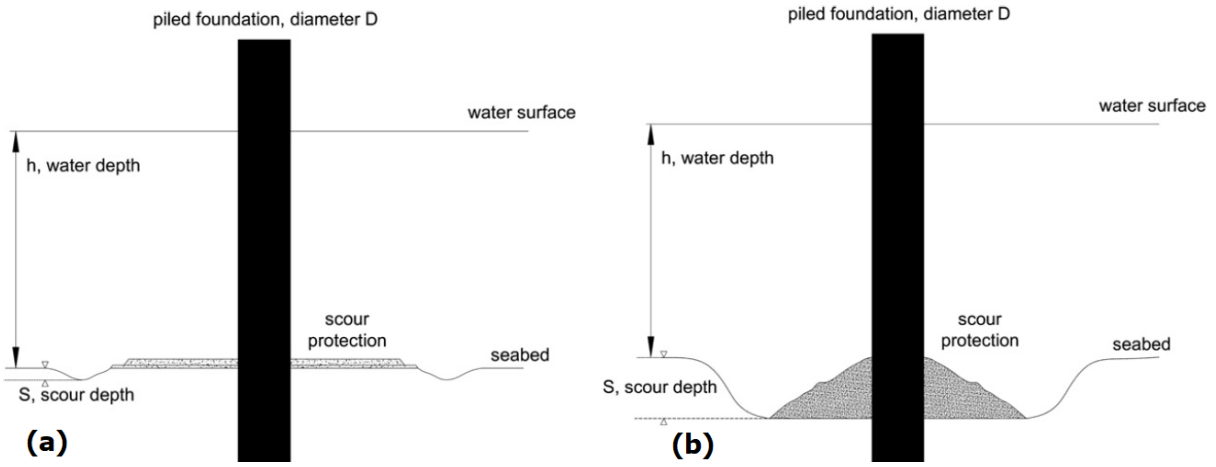

Figure 1.3 (a) Scour protection layer that is installed before the pile, (b) Scour protection or mitigation measure that is installed after the pile and the formation of the scour hole. Whitehouse et al., 2011

In the offshore wind farms that are investigated in this review the most common scour protection, that is employed, is the rock armor. According to Whitehouse et al., 2011, a standard procedure is followed for the protection of the seabed against scour. Firstly, a preparatory layer is installed in the seabed that contains gravel or small rocks. This layer acts as a filter between the seabed and the main layer of the protection. Then, after the aforementioned filter layer is installed, large blocks of rock are placed above the filter, composing the main resistance against erosion (Figure 1.3 (a)). They are certain criteria about the composition of the scour protection as well as the method of depositing it, but in the real ocean conditions it is often not possible to apply these regulations explicitly. As a result, in each certain case, it is common to have a case-specific protection layer. In cases that scour has occurred and it is more severe than expected during the design phase, mitigation measures are necessary to avoid possible failure of the monopile. A most common practice is to fill the scour hole that has been formed with a widely graded rock around the monopile (Figure 1.3 (b)). In this way, it is possible to stop or at least limit the scour phenomenon and offer some extra lateral resistance to the pile, by increasing its stiffness.

One important aspect that needs to be discussed about the scour protection is the edge scour. More specifically, when the protection layer is installed and works properly, there is no scour in the seabed below the layer. However, in the edges, the protective layer cannot prevent scour from happening. Therefore, it could be said that in a way, the scour protection transfers the scour holes away of the monopile. In this way, if there is a sufficient area without scour surrounding the pile, the soil can offer enough lateral resistance against the cyclic loading. However, if the edge scour becomes too extreme, it may lead to instability of the soil protected by the blocks of rock, as large slopes may be formed in the edges of the scour protection layer.

To better examine the characteristics of the protection scour layer and the mitigation measures used, certain case studies will be mentioned, as they are introduced in the work of Whitehouse et al., 2011. More specifically, in the Horns Rev OWF, 4.25 outside-diameter monopiles have been founded in a fine to coarse sand. Prior to the placement of the pile, a protective layer has been set in the field, which was composed of two layers. The first one was a filter layer of 0.5m thickness and the material used was a median rock with particle size d_{50}=0.10m. The second layer contained the rock armor, with a thickness of 1.5m, that was composed by rock material with particle size d_{50}=0.40m. The protective layer was placed in a radius of about 2.2D from the center of the monopile. The edge scour that was observed was about 0.5m which can be approximated as 0.15D or 1/3 of the protective layer. Almost the same characteristics of the protection layer are observed in the Egmond aan Zee OWF. More specifically, the protection layer is composed of the filter one, with a thickness of 0.4m and nominal rock size of 0.05m, and the armor layer, with a thickness of 1.4m and a nominal rock size of 0.40m. A small difference though with the previous case study is the fact that the filter layer was placed in a larger radius (2.60D) around the center of the monopile, while the body armor had a radius of about 2.0D. However, it is clear that in both cases the same principles have been followed in the design.

An example in which the scour hole has been filled with material after it has been formed is the case of Arklow Bank OWF, where a 5m diameter monopile has been installed. According as before to Whitehouse et al., 2011, in this case a scour hole has been formed with a depth of about 1.0D. Then material fill was dumped in this hole which was composed of graded rock and gravel in order to limit the scouring of the soil and increase the stiffness of the system of the soil and monopile. After, the scour was filled, secondary scour took place but in a lower rate, mainly causing erosion of the soil in the edges of the dumped material. After a certain period of time, the scour in the edges was about 1.5D deep while close to the pile, the scour phenomenon has been limited in an efficient way.

Matutano et al., 2013 investigated extensively the scour development that is proposed by most authors or that has already been applied to existing offshore windfarms. According to them, in the first offshore constructions, it was more preferable to deal with the scour by increasing the length or the diameter of the pile instead of the scour protection, although nowadays a different philosophy is applied, as scour protection has become more efficient and attractive from an economic point of view. The most common materials that are used, are large stones and rocks as they are a low-cost material and are generally easily available to the offshore fields. Of course, these materials may be hard to be dumbed in a proper way to the field around the monopile and are susceptible to damage in case of extreme waves or currents, but as a total they are characterized as the most efficient scour protection measure, including the economic point of view. As already mentioned, the standard design of the protection scour is composed by one filter layer with small sized rocks and the main armor that contains large-sized stones and rocks. The rocks in the main armor must be large enough to withstand the forces that will be applied to them by the currents and the waves, along with the cyclic loading of the monopile due to the function of the wind turbine. According to Matutano et al., 2013 the scour protection is characterized by three parameters, the stone size d_{50}, the diameter and the thickness of the protection layers. These characteristics are presented in the tables below for a series of offshore wind farms. It needs to be stated though that not all the information is known, as in some cases there is no distinction between the filter layer and the rock armor layer, or no data about the thickness of the protection.

Table 1.1 Rock size & thickness of the scour protection layers in different OWFs. Matutano et al., 2013

Name	**d_{50} [m]**	**Thickness [m]**
North Hoyle	0.3	Unknown
Egmond aan Zee	0.4	1.4(armor)
Thornton Bank	0.35	0.7
Horn Rev	0.2 (filter) & 0.4 (armor)	0.5 (filter) & 0.1 (armor)
Scroby Sands	0.15	Unknown
Arklow Bank	0.425	Unknown

Table 1.2 Recommendations in literature for the diameter of scour protection. Matutano et al., 2013

Author	**Diameter of Scour Protection**
Bonasoundas (1973)	2.5D-4.5D
Hjorth (1975)	2.5D
Breusers & Raudkivi (1991)	3D-4D
Hoffmans & Verheij (1997)	2.5D-4D
Melville & Coleman (2000)	3D-4D
May (2002)	2D

As it is obvious from the data in the tables above there is a scatter in all the three basic parameters of the scour protection. Regarding the size of the rocks and the thickness of the material layer though this may be attributed to the fact that there are not clear data for all the OWFs. Therefore, the rock size

might have occurred as the median size of the filter and the armor layer for instance. However, regarding the diameter of the scour protection the range of the values is between 2D to 4.5D which is a relatively high scatter but can be attributed to the different conditions (currents and waves) in the offshore fields that the monopiles have been installed, demanding different-sized scour protections.

1.1.3 Scour effect on stiffness and lateral capacity of the soil-monopile system

Yasser E. Mostafa, 2012 performed numerical investigation of the effect of the scour in the lateral capacity of a monopile in sandy soils. More specifically he investigated the effect of both the depth and the type of scouring on the lateral soil response, using the software programs PLAXIS & LPILE. Parametrical analyses included four different scour depths (1.0, 1.3, 2.0 & 3.0D) and all types of scour, the local (wide and narrow) and the global one, as it can be seen in Figure 1.4.

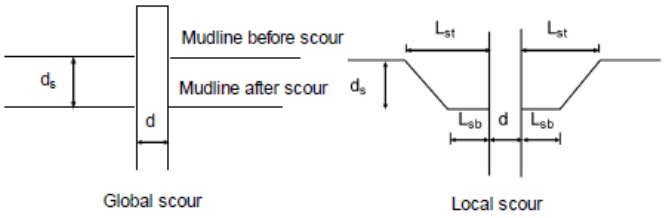

Figure 1.4 Design of the global and the local scour type that have been used in the analyses. (Yasser E. Mostafa, 2012)

The ultimate lateral capacity of the pile when global scour is simulated was significantly lower (about 50%) comparing to the no scour case. In addition, the global scour case is more sensitive comparing to the local scour case, as the ultimate lateral capacity of local scour was larger about 50% to 70% depending on the depth of the scour. On the other hand, the shape of local scour had a smaller influence in the results, as the capacity was slightly larger in the narrow scour hole. The increase in the scour depth had a great influence in the pile head displacements, as in the global scour the increase in the pile deflection exceeded the no-scour case by 150%. Finally, it was stated that the effect of the scour hole was more intense when the piles have been subjected to relatively large lateral loads. This could be attributed to the non-linear response of the soil-monopile system in high loads, as the soil would reach the plasticity branch due to large deformations.

Qi et al., 2016 performed centrifuge experiments to investigate the scour effect in the p-y curves for shallowly embedded piles in sand. They have performed tests to investigate the scour effect both for local and global scour type. It needs to be noted that for the global scour case, the piles had the same embedded length but different over-consolidation ratio. The p-y curves have been derived with the methods proposed by Wang & Qi, 2008. They have concluded in accordance with previous research that the scour, either global or local, reduces significantly the stiffness of the soil-monopile system. The most interesting result they have observed though it that the API method led to a stiffer behavior of the pile head comparing to the one that has been measured in the experiment, indicating that the API regulations overestimate the soil lateral capacity. Regarding the p-y curves, the different OCR ratio in the set of global scour experiments had no actual influence in the curves which are mainly affected by the soil surface level and the embedded length, that was common in all global scour tests. For the local scour set of experiments though, an interesting finding was observed, as the p-y curves have been affected only in the shallow depths, close to the scour hole, while near the tip of the pile, the p-y curves were actually the same as in the case of no scour. In the shallow depths, the p-y curves after the scour hole has been formed presented more stiffness than the ones in the no scour case. This can be attributed to the fact that in the case of scour, more soil resistance has to be mobilized in the same level comparing to the one in no scour case, as less embedded pile length is available for reaching an equilibrium.

1.2 State-of-the-Art in Scouring Process

1.2.1 API (American Petroleum Institution) Method & Regulations

Current practice follows recommendations from the API regulations to account for the soil-monopile interaction, based on the p-y curves. The basic concept that is adopted for the aforementioned curves is the Winkler type approach. Uncoupled and non-linear springs are employed in the whole embedded length of the monopile, relating the soil resistance p that is induced by a lateral pile displacement y in any depth. The characteristics of each spring are unique, rendering this method rather popular as it can stand for the heterogeneity of the soil, by only modifying the spring properties. The mathematical relation between the soil resistance and the pile deflection is the following formula:

$$E_p I_p \frac{d^4 y}{dz^4} - p(y) = 0 \qquad \textit{Eq. (1)}$$

The parameters E_p and I_p stand for the pile's Young modulus and moment of inertia respectively. The initial development of the p-y curves can be attributed to Lymon C Reese & Matlock, 1956. However, the oil and gas industry led to the evolution of the p-y curves in the 70s and 80s where the demand for offshore piles has increased significantly. Therefore, experiments have been performed, a lot of them in full scale, to be able to predict the pile response both for static and cyclic loading. Based on the research of Lymon C Reese et al., 1974, McClelland & Focht, 1980 and O'Neill & Murchison, 1983, new recommendations and standards have been published for offshore pile designing (API 1993).

In Figure 1.5 the p-y curves for sandy soils as proposed by Lymon C Reese et al., 1974 are presented. This graph is the base of the modern approach in the API (2005) regulations in the p-y curves formation. The model can be distinguished in three areas, the first one where an elastic behavior is adopted, the third one where the curve reaches its plastic branch and the middle one that smoothly connects the elastic and plastic area. It needs to be stated that the parameter b in Figure 1.5 is the pile diameter, and it is quite interesting to observe that the plastic branch is captured at a small displacement of 0.0375 times the diameter.

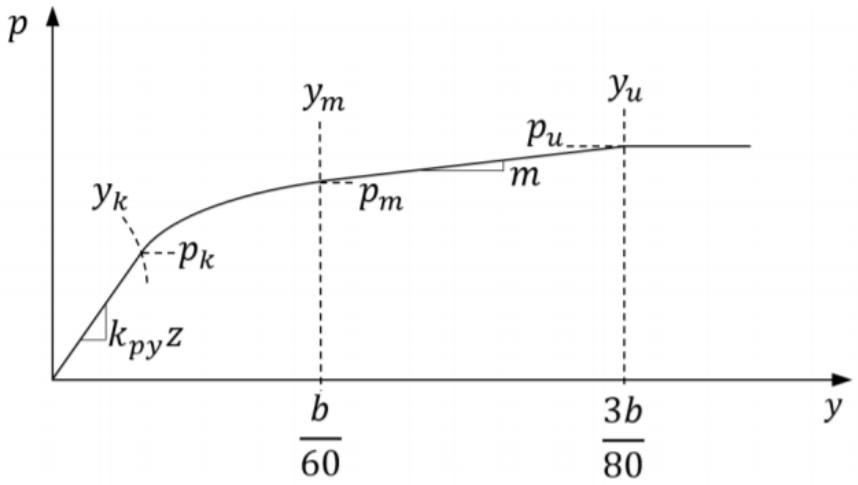

Figure 1.5 p-y curves for sandy soils as proposed by Lymon C Reese et al., 1974.

The new API regulations (2005) for deriving the p-y curves for offshore piles in sandy soils, propose the following equation:

$$p = Ap_u \tanh\left(\frac{kH}{Ap_u} y\right) \qquad \textit{Eq. (2)}$$

The aforementioned equation, can be applied to both static and cyclic load conditions. The distinction between the two cases is performed by the parameter A, which depends on the depth and the pile

diameter for static load, and is given the value of 0.9 for cyclic loading conditions. The term p_u corresponds to ultimate lateral capacity of the soil at each depth, based on empirical correlations with the eternal friction angle and the depth. The subgrade modulus k is included in the equation and is also based on empirical charts that correlate its value with the friction angle, the density and the water table.

The API method's initial applications had a low rate of failure which made the method well known and popular. However, when the same regulations applied to offshore monopiles the method proved not to be equally efficient. Verdure et al., 2003, Achmus et al., 2009, LeBlanc et al., 2010 and Qi et al., 2016 applied both numerical and experimental investigations on the response of a soil-monopile system under monotonic and cyclic loading. They all reach the conclusion that the API method in general over-estimated the soil strength, especially in small deformations implying a much stiffer behavior of the soil-monopile system than in reality. In addition, it failed to fully capture the mechanisms that offer the soil resistance during the deflection of the pile, both in static and cyclic conditions. This can be attributed to the fact that important aspects of the behavior of the offshore mono-piles are not taken into account by this methodology. First of all, the p-y curves are based on empirical charts that have been derived for long flexible piles. However, the monopiles that are the foundation type for over 75% of the windfarms, as already stated, are in general short rigid piles. On the same context, the API method has been based in small diameter piles of less than 3.0m, while the typical offshore monopile has a diameter of at least 4.5m. The high rigidity of the monopiles means that the pile will not actually deform in its axis, but instead it will rotate as a rigid body through a steady rotation point, usually from 2/3 to 3/4 of the embedded length. Consequently, in the bottom of the pile, under the rotation point, the toe-kick will appear, which indicates that the toe will move to opposite direction of the top of the pile to reach the necessary equilibrium. This small detail is crucial, as it clearly states that the whole pile needs to mobilize soil resistance, while the slender piles in which API method is based, will activate only a part of their embedded length that will deform towards the same direction and will act as cantilever. Therefore, the actual behavior of the typical rigid monopile cannot be captured by the API, as their mechanism for equilibrium against displacements is completely different from the slender, flexible piles.

Another problem in the current method is that the derived p-y curves focus on the evaluation of the ultimate capacity of the soil. In reality though, the ultimate lateral capacity is not always the case in monopiles as the interest is focused in small deformations caused by the static or cyclic load in order to ensure that SLS are satisfied and the functionality of the wind turbine is not obstructed. Therefore, the initial stiffness of the soil-monopile system is rather important for small strains and the API seem to over-estimate in a high the degree this parameter. Last but not least, focusing on the cyclic conditions, the p-y curves in the API method have been derived for a small number of cycles of about 200 which is not indicative for the lifetime of the monopile in offshore conditions which will be loaded with a great number of cycles of at least 10000 cycles. Obviously, this fact is not completely relevant with the static loading, but it is indicative of the certain scientific gap between API and offshore monopiles in real conditions.

1.2.2 Current State-of-the-Art

The inadequacy of the API to predict in a reliable way the response of the rigid monopiles in offshore conditions has rendered them as outdated in the certain topic. Despite that though, certain recommendations of the API method are still adopted by the engineer firms during design. However, the design procedure for a typical offshore monopile is also based on standards from International Electrotechnical Commission (IEC), Det Norske Veritas (DNV) and Germanischer Lloyd (GL). The IEC is an international organization that provides standards for the electrical and electronic technologies, along with the ones related to them. Marine wind energy is a sector of interest for IEC and through the IEC61400-3 (Wind turbines: Part3: Design requirements for offshore wind turbines;2009) assesses the external conditions at an offshore site and specifies vital designing requirements for the integrity of the wind turbines during their lifetime. It mainly focuses on the structural and the electrical components of the turbine, but along with the IEC 61400-1 (Wind turbines: Part 1: Design requirements) offers certain

guidelines for the foundation of the wind turbines and the interaction between soil and monopile which is the point of interest on this report.

Det Norske Veritas (DNV) and Germanischer Lloyd (GL) were registrar and classification organizations in Norway and Germany respectively. They have now emerged in the DNV GL, being the largest organization in the field, offering services to maritime, renewable energy and oil & gas sectors. Through the "Design of Offshore Wind Turbine Structures. Technical Report, DNV; 2014 (DNV-OS-J101)" and "Guideline for the Certification of Offshore Wind Turbines; 2012, GL" the DNV GL offers guidelines for the adequacy of the monopile design against ultimate limit state (ULS), serviceability limit state (SLS) and fatigue limit state (FLS) which is connected with the cyclic loading effects. More specifically, they provide design principles, load and resistance factors, materials, foundation design and anything else relevant to a proper and efficient design of an offshore design. It needs to be noted that the current state of art set as a limit for the ultimate limit state a horizontal deformation of the pile in the soil surface equal to 0.1D. Of course, this deformation does not actually cause failure from a collapse point of view, but it indicates that the monopile is moving towards a not-return situation, rendering the wind turbine completely non-functional. The scour phenomenon is also included in the regulations, as they propose formulas to predict the hole formation and its geometry, along with the time needed. However, they clearly indicate that scour formation is a case-sensitive phenomenon as it is greatly influenced by the combination of waves and currents along with the soil properties in a specific area and therefore the aforementioned formulas should be cautiously used. Regarding the scour effect in the soil-pile system's stiffness and lateral capacity the DNV GL propose certain modifications in the p-y curves as proposed by API method, by mainly reducing the ultimate soil resistance at each depth. However, it is clearly stated that the p-y curves have been extracted for the slender piles and therefore may not be applicable in the rigid monopiles and that the p-y curves method is suitable for the defining the ultimate limit state.

The existing regulations take into a lot consideration the effect of the scour formation in the behavior of the offshore monopile. They insist on evaluating its impact on the reduction of the soil resistance and the stiffness of the soil-monopile system, but they do not offer a recommendation or a formula for this topic. This scientific gap is expected to be covered by this report, by producing a relation between lateral capacity, stiffness and scour characteristics (depth and type).

1.3 Problem Statement & Objectives

The research question that this study attempts to answer is what is the effect of the scour formation (type and depth) and scour protection in the lateral response (capacity and stiffness) of a monopile in offshore conditions under a monotonic load. To focus on this problem, certain other parameters should be eliminated by investigating their own effect in the lateral capacity of the soil-monopile system. Therefore, the objectives of this study are presented in the list below:

[1]. What is the effect of the vertical dead load in the lateral capacity of the monopile?

[2]. What is the effect of the incremental filling ratio of the monopile (soil plugging inside the pile) in the lateral capacity?

[3]. Which scour type is the most critical in terms of soil resistance's reduction? The scour type effect is significant or negligible comparing to the scour depth effect?

[4]. Scour protection contributes to the soil-pile system's lateral resistance? Is this contribution large enough to be important for the design phase or should not be taken into account?

The main focus of this study is given in answering the second questions [3] and [4], as the current literature has not provided yet an explicit view on these statements. Therefore, the largest part of the simulations is conducted towards this direction. However, the effect of the vertical load in the lateral capacity is rather interesting as in the literature there are many results that contradict to each other. Hence, the effect of the dead load cannot be safely predicted beforehand without any analyses.

Chapter 2

Methodology

The aim of this project is to evaluate the impact of the scour formation and scour protection measures in the stiffness and the lateral capacity of a typical offshore monopile. This investigation is performed by numerical analyses in the finite element code of PLAXIS 3D. The numerical model that is used along with the soil parameters are described analytically below, along with the sequence of the analyses in order to reach the desired conclusions.

2.1 Model Geometry

In Figure 2.1 the model developed in PLAXIS is presented, which was used for the numerical investigation of the scour formation and protection effect in the lateral capacity and stiffness of the soil-monopile system. It needs to be stated that the numerical model was based on a centrifuge model that has been created to simulate the same problem. Therefore, the dimensions of the numerical model, including the soil, the pile etc. have been chosen so as to match the prototype scale dimensions derived by the centrifuge experiments. In Appendix A the format of the centrifuge experiment is briefly presented.

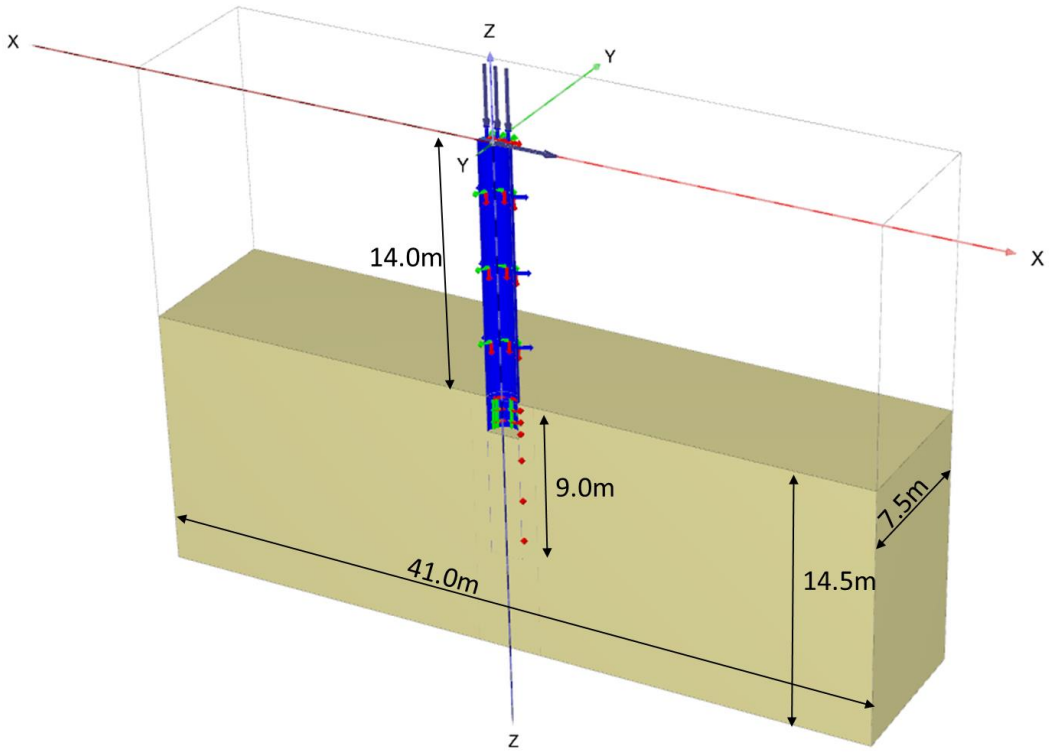

Figure 2.1 PLAXIS model that is used for the simulations.

The model is a 3-D symmetrical one, as modelling a single pile that is subjected into a certain loading is one of the most typical symmetrical problems. In this way, the computing resources and the time needed for each analysis can be reduced considerably. The dimensions of the model have been chosen

in a way that will be equal to the prototype of the strongbox that has been used in the centrifuge. Obviously, the values in the perpendicular direction of the symmetry surface are reduced in half. Therefore, the exact dimensions of the model are 41x7.5x14.5m. The width and the height of the model may not be large enough to eliminate possible boundaries effects. However, it is intended to have a comparison between the numerical and the experimental results in a future report, therefore it was decided to keep the possible error caused by the boundary effects in order to have the exact same conditions in physical and numerical modelling. On the same context, the model that has been developed contains dry sand to match the centrifuge modelling. This is not expected to be crucial, though, as the sand presents a drained behavior and hence no excess pore pressures are developed during the loading. For this reason, it is quite common to use dry samples in centrifuge experiments, as saturated samples are quite difficult to be dealt with. Consequently, all the simulations that are performed in the current PLAXIS model are dry.

The pile has a diameter of 1.8m and it is embedded 9.0m deep into the soil. The diameter is relatively small comparing to the ones in the real-case projects, as a typical diameter of an offshore monopile is around 5.0 to 6.0meters. However, the ratio L/D in the numerical model is equal to 5, which is the same ratio that is met in most offshore wind farms. Therefore, from this point view, it is valid to consider the pile's dimensions to be representative of the real conditions.

As it has already mentioned, the numerical modelling was developed to be as close to the centrifuge model as possible. For this reason, after some preliminary analyses that are presented in Appendix B it was decided not to use an interface. This choice is the outcome of two factors. First of all, the pile that was used in the physical modelling is really rough in its exterior part due to some strain gauges that are placed there. Consequently, it was considered to be more realistic to have the same friction in the soil-pile interface and the soil itself. The second reason has to do with the nature of the problem. More specifically, as it can be seen in the preliminary analysis in the Appendix B, using an interface with reduced strength properties and one with the original strength properties has no actual effect on the results. Therefore, no interface has been used to simulate the monotonic push.

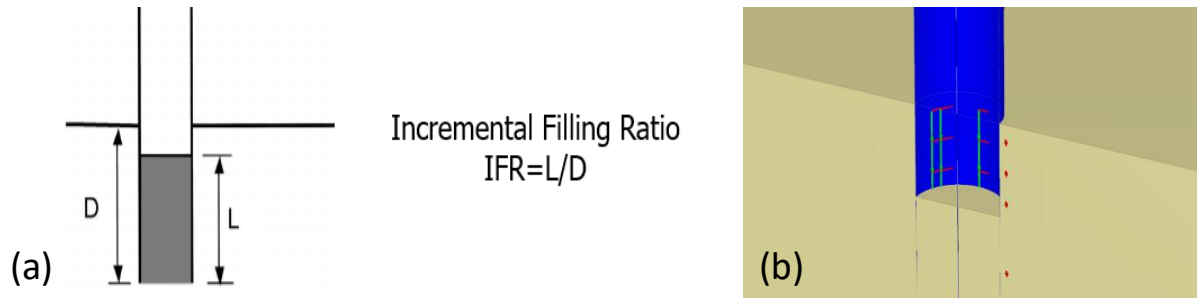

Figure 2.2 (a) Incremental Filling Ratio definition. (b) IFR in the PLAXIS model

The incremental filling ratio (Figure 2.2a) defines the plugging that has occurred in the pile during its driving in the soil. Since it cannot be known beforehand what the soil plugging might be, a preliminary analysis has been performed to define its importance (Appendix B). As it was shown, this term has no actual influence in the lateral soil capacity of the monopile, therefore it was decided that the pile in its interior should be filled with soil up to 1.0D distance from the current soil surface in each analysis, as a realistic assumption (Figure 2.2b).

In Figure 2.3 the upper part of the pile is presented. In all the analyses, a vertical dead load is simulated, which represents the weight of a typical wind turbine, that is about 3.0MN. This load is simulated as a surface load in a plate created in the top of the pile. In the same plate a prescribed displacement is applied equal to 1.0m to investigate the lateral response of the soil-monopile system. To eliminate any undesired error due to deformation of the upper plate by the vertical load or the prescribed displacement, a high stiffness was given to this plate. More specifically, it is 0.5m thick with an elasticity modulus of 200GPa, rendering it completely stiff for the loading that is applied. In addition, the unit

weight of this plate is set equal to 0, in order not to cause an extra vertical load to the pile due to its own weight. Therefore, the upper plate serves only as a means for applying the desired load and displacement.

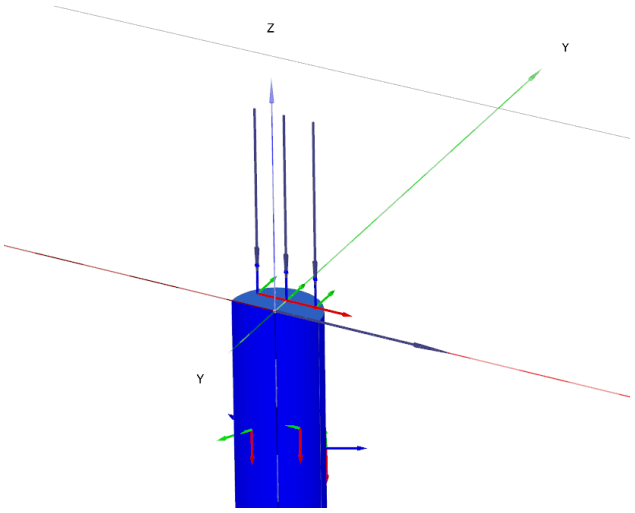

Figure 2.3 Top of the pile, where the dead vertical load and the prescribed displacements are applied.

In Figure 2.4, the meshing of the numerical model is depicted. The pile and the surrounding soil are densely meshed in an area of about 2.0D, while it gradually gets coarser towards the boundaries. Having an even more dense mesh was tried in initial test analyses, but the accuracy of the results has only slightly increased, requiring though extremely more computational time. Therefore, the negligible increase in the results' accuracy was considered to be non-efficient as one single analysis would require more than twice the time comparing to the final mesh of Figure 2.4 that was used in the current project.

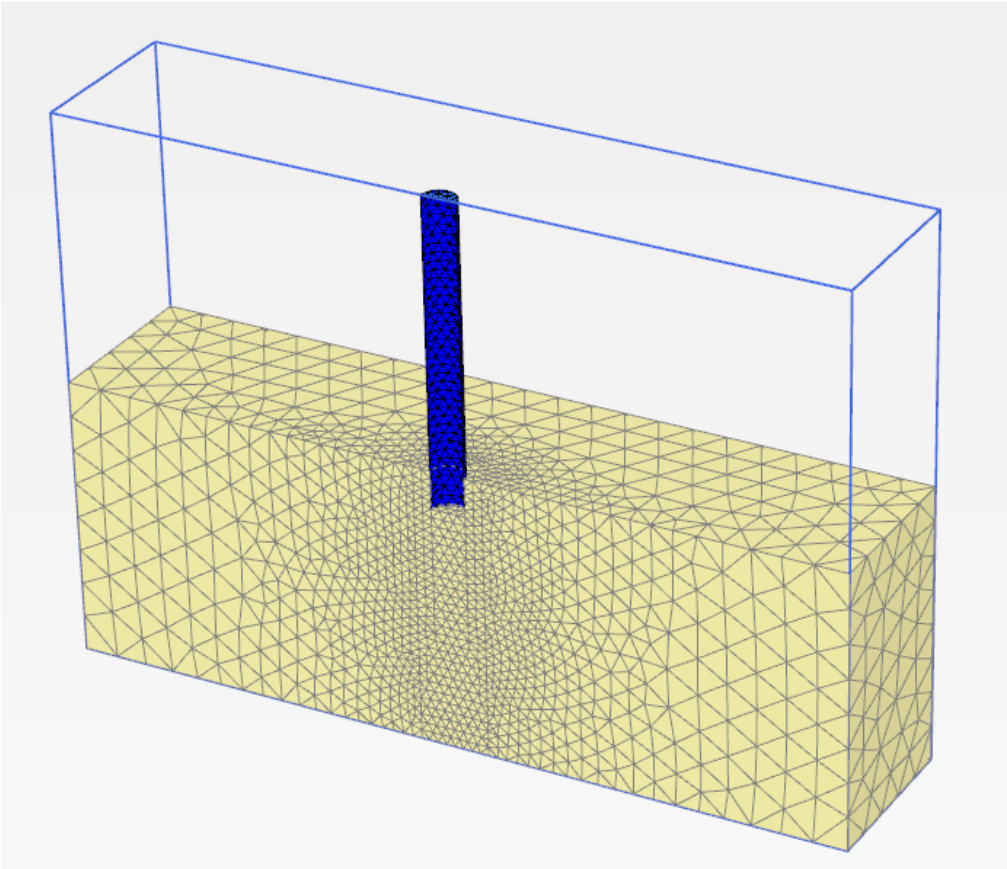

Figure 2.4 Meshing of the PLAXIS model, which includes the pile and the soil.

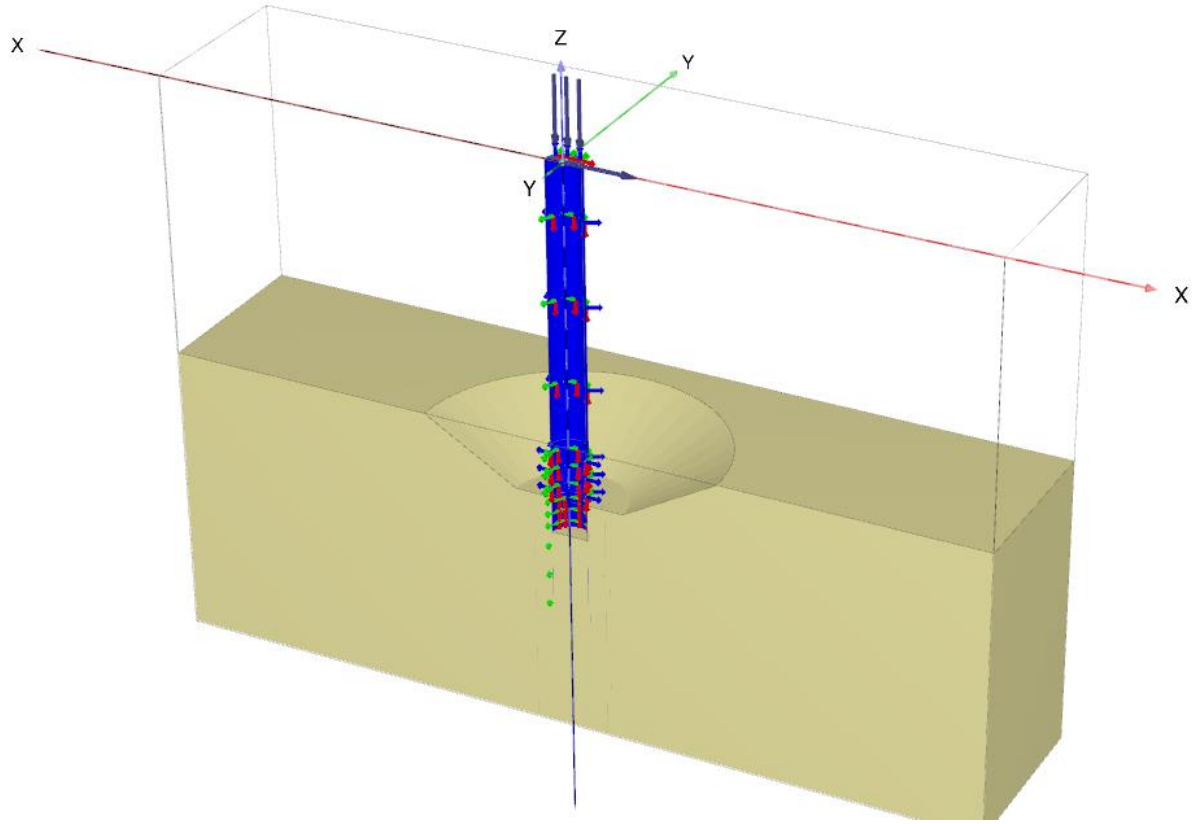

Figure 2.5 Scour formation simulation on the PLAXIS model.

In Figure 2.5 a certain case of scour formation is depicted. More specifically, a wide type of scour is presented, for a depth of 1.5D. In all the cases of the wide type of scour in the current report, the horizontal area around the pile has a length of 1.0D from the edge of the pile to the beginning of the slope. The inclination is constant in both wide and narrow type of scour and is equal to 30° (Figure 2.6). As it can be seen in Figure 2.5, there is an area inside the pile in which no soil exists for a depth of 1.0D. The same pattern has been followed in all the scour simulations.

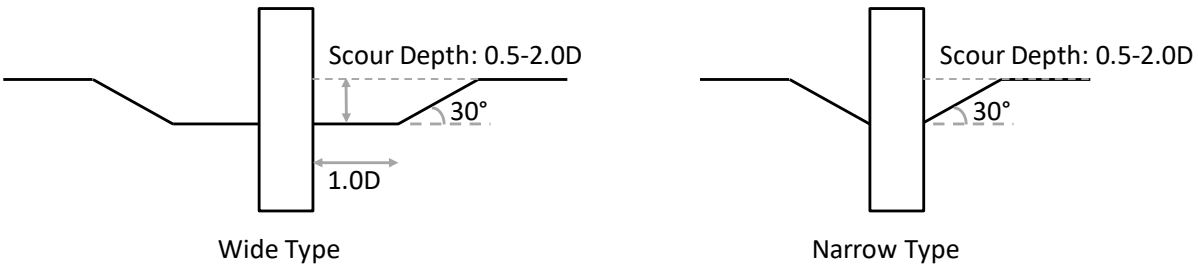

Figure 2.6 Scour formation geometry in the PLAXIS simulations.

In Figure 2.7 the scour protection is presented as simulated in PLAXIS analyses. The diameter or length of the scour protection that is investigated in this report is 3.0, 5.0 and 7.0 times the diameter of the monopile. The possible contribution of the scour protection in the lateral capacity and the stiffness of the soil-monopile system occurs due to the increase of the overburden pressure around the monopile. More specifically, due to the nature of the material used as scour protection it is safe to assume that there will not be a constant contact between scour protection and monopile. Therefore, only the extra pressure that these materials offer to the surrounding soil of the pile is simulated. The pressure that is applied in the red surface in Figure 2.7 is equal to 15kPa. This value has occurred as the typical scour

protection layer is 1.0m thick and the effective unit weight of the rock material that is used is about 15kN/m^3. The reason for opting for the effective unit weight is to simulate the pressure that the scour protection would offer in a real case situation in offshore conditions.

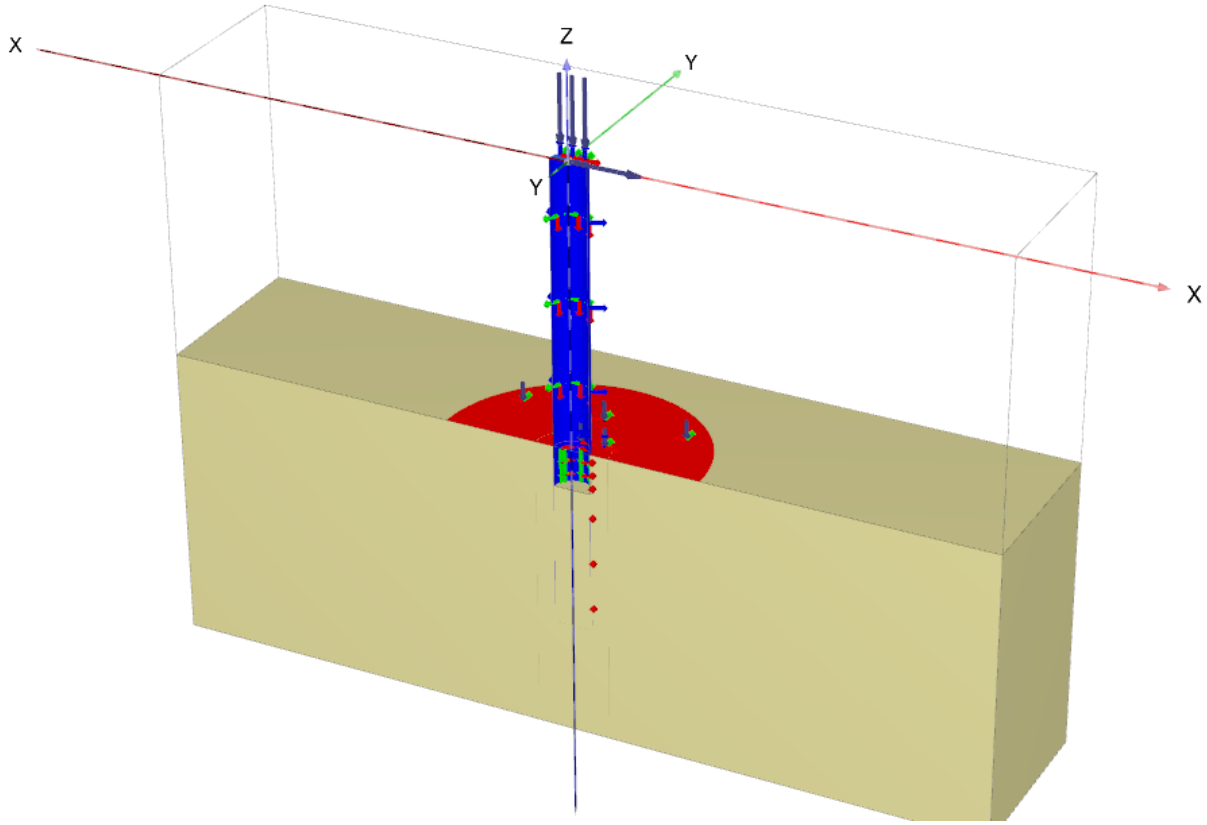

Figure 2.7 Scour protection simulation (red surface).

2.2 Constitutive Model

The hypoplastic model has been chosen as an appropriate constitutive model for the specifications of the problem investigated. The main characteristic of this model is the relation between stress and deformation with a single equation, without distinguishing elastic and plastic region. It can simulate both hardening and softening behavior of the soil, as it is an expansion of the critical state theory. In addition to this, stiffness is calculated as a combination of both soil density and mean stress which allows for a more realistic soil behavior. Its main disadvantage is the undrained behavior, as it does not seem to capture it accurately, by comparing model results and laboratory tests. In this project, though, undrained behavior cannot occur as all the analyses are performed in dry sand. In general, it is considered a difficult model to be adopted in analyses as it contains a lot of parameters, which do not always have a clear physical meaning. Therefore, it is quite hard to validate the model into a certain problem. However, the advantages of this model in simulating a realistic soil-monopile system's response overshadow possible difficulties, rendering it as highly sophisticated model. The version of hypoplasticity that is going to be used is the von Wolffersdorff, 1996 version, with the addition of the intergranular strain concept, which is briefly described below.

2.2.1 Von Wolffersdorff's Version of Hypoplasticity

Von Wolffersdorff, 1996 version of the hypoplasticity with the addition of the intergranular strain concept is the basis of hypoplastic model. Its general form is the following:

$$\dot{T} = F(T, e, D) \qquad \textit{Eq. (3)}$$

with $\dot{T}$ being the stress rate, depending on Cauchy stress and void ratio, e being the void ratio and D being stretching tensor. The equation of the void ratio state variable is:

$$\dot{e} = (1 + e)trD \qquad \textit{Eq. (4)}$$

The constitutive equation as proposed by von Wolffersdorff, 1996 is the equation 5:

$$\dot{T} = \frac{f_s}{tr(\hat{T} \cdot \hat{T})}[F^2 D + a^2 \hat{T} tr(\hat{T} \cdot D) + f_d a F(\hat{T} + \hat{T}^*)\|D\|] \qquad \textit{Eq. (5)}$$

The term F is a function of the deviatoric stress ratio tensor. The terms $(\hat{T}^*)$ and f_s can be described as:

$$f_s = f_e f_b = \frac{h_s}{n}\left(\frac{1 + e_i}{e_i}\right)\left(\frac{e_i}{e}\right)^{\beta}\left(\frac{-tr(T)}{h_s}\right)^{1-n}\left[3 + a^2 - \sqrt{3a}\left(\frac{e_{i0} - e_{d0}}{e_{c0} - e_{d0}}\right)^{\alpha}\right]^{-1} \qquad \textit{Eq. (6)}$$

$$\hat{T}^* = \hat{T} - \frac{1}{3}I \qquad \textit{Eq. (7)}$$

In the equation 6, the term h_s is the granular hardness which has stress units. In essence it is a reference pressure and should not falsely misinterpreted with the strength of the soil grains. The factors f_b, f_d and f_e are used to describe the density dependence and the pressure dependence as proposed by Kolymbas, 1985. These factors separate density and pressure dependence from the response function F. The hypoplastic model has been based to the Drucker/Prager model and the Matsuoka/Nakai yield criterion. Regarding the void ratio terms, three characteristic values are implemented in the model, the maximum void ratio (e_i), the minimum void ratio (e_d) and the critical void ratio (e_c). The aforementioned term α stands for the failure by the Matsuoka/Nakai criterion with the equation 8:

$$a = \sqrt{\frac{3}{8}}\frac{(3 - sin\varphi_c)}{sin\varphi_c} \qquad \textit{Eq. (8)}$$

The term φ_c is the residual friction angle. According to Bauer, 1996, all the state values of the void ratio are reducing with the mean pressure which is defines as:

$$p_s = -tr(T/3) \qquad \textit{Eq. (9)}$$

The void ratio will reach the values of e_{i0}, e_{d0} and e_{c0} when the mean skeleton pressure (p_s) is almost vanished, while for really great values of p_s will approach a zero value. The relationship of the void ratio states with the mean skeleton pressure is the following:

$$\frac{e_i}{e_{i0}} = \frac{e_d}{e_{d0}} = \frac{e_c}{e_{c0}} = \exp\left[-\left(\frac{3p_s}{h_s}\right)^n\right] \qquad \textit{Eq. (10)}$$

2.2.2 Intergranular Strain Concept

The original hypoplastic models that have been developed, have been characterized by inaccuracies during loading in small stress cycles, as excessive accumulation of deformations has been observed leading to unrealistic large displacements. Atkinson et al., 1990 and Puzrin & Burland, 1998, proved that soil response is characterized by highly inelastic and history dependent behavior in small strain loading. Niemunis & Herle, 1997 produced a state parameter, the intergranular strain (h). This state variable considers the deformation of the interfaces of the grains and the change in their positions with each

other for small stain loading, dealing with the problem mentioned in the original versions of hypoplasticity.

The stiffness calculation is the main parameter affected by the intergranular strain concept, comparing to the previous versions of the model. To be more specific, the intergranular strain tensor is driven by the difference in the direction of the actual strain rate $\dot{\varepsilon}$ and the intergranular strain rate $\hat{h}$ along with the value of the tensor h, as shown in the equations below:

$$\dot{h} = \begin{cases} (\Im - \hat{h} \times \hat{h}\rho^{\beta_r}) : \dot{\varepsilon} & for \quad \hat{h} : \dot{\varepsilon} > 0 \\ \dot{\varepsilon} & for \quad \hat{h} : \dot{\varepsilon} \leq 0 \end{cases} \qquad \textit{Eq. (11)}$$

$$\hat{h} = \begin{cases} h/\|h\| & for \quad h \neq 0 \\ 0 & for \quad h = 0 \end{cases} \qquad \textit{Eq. (12)}$$

The intergranular strain tensor's magnitude is calculated as $\rho = \|h\|/R$, with R being the intergranular strain radius. The general interpolation of the stiffness M that is performed for the relative angle θ between the current strain rate $\dot{\varepsilon}$ and the recent strain history is the following:

$$M = [\rho^x m_T + (1 - \rho^x) m_R]\mathcal{L} + \begin{cases} \rho^x (1 - m_T)\mathcal{L} : \hat{h} \times \hat{h} + \rho^x N \times \hat{h} & for \quad \hat{h} : \dot{\varepsilon} > 0 \\ \rho^x (m_R - m_T)\mathcal{L} : \hat{h} \times \hat{h} & for \quad \hat{h} : \dot{\varepsilon} \leq 0 \end{cases} \qquad \textit{Eq. (13)}$$

The terms m_T and m_R correspond to the increase of the stiffness after a full load reversal and to the increase of the stiffness after a 90° change in the direction of the strain path respectively.

2.3 Material Properties

In the numerical modelling the sand that is simulated is the Geba sand, as this is the one used in the centrifuge tests. The Geba sand is a uniform silica sand, that is generally composed of rounded and sub-angular particles. According to de Jager et al., 2017, this type of sand has a mean grain size of d_{50}=0.12mm, which indicates a very fine sand, very susceptible to liquefaction in small to medium relative densities. Azua Gonzalez, 2017 in his thesis used the Geba sand and through experiments performed in the laboratory (oedometer tests), he defined the properties of this sand. More specifically, the three characteristic values of the void ratio, the maximum one (e_i), the critical one (e_c) and the minimum one (e_d) are respectively 1.28, 1.07 and 0.64. The void ratio that corresponds to the relative density of 80% based on the aforementioned values can be calculated as 0.73. The mean specific gravity Gs was also defined as equal to 2.67, which produces a dry unit weight of 15.2kN/m^3 and a saturated one of 19.3kN/m^3. As it was presented above, the hypoplastic model requires a certain number of parameters in order to be defined. The calibration of these parameters was based on laboratory tests by David Masin, in his report issued for the Royal IHC. David Masin is considered to be an expert in hypoplastic model as he has a large contribution in the evolution of the model. Therefore, based on his test for the Geba sand, the calibration of the model has been completed and is presented in the following subchapter. It needs to be noted that the report containing the tests of Masin is confidential and therefore it will not be presented in this report.

2.3.1 Soil

The parameters for the hypoplastic model that have occurred by the calibration of the model are presented concisely in the Table 2.1. To be more specific, the parameters are distinguished into two parts, the von Wolffersdorff, 1996 version' ones and the intergranular strain concept's ones.

Table 2.1 Hypoplastic model parameters after the calibration of the PLAXIS model

von Wolffersdorff's hypoplastic model parameters							
φ_c	h_s	n	e_{d0}	e_{c0}	e_{i0}	α	β
34	2500MPa	0.30	0.640	1.070	1.280	0.11	2.0
Intergranular Strain Concept							
m_R		m_T	R_{max}		β_r		χ
5.5		3.9	0.0001		0.3		0.7

2.3.2 Pile

The pile that has been modelled for the numerical analyses has the same characteristics as the one in the centrifuge. Therefore, the aluminum elasticity modulus was adopted, while the rest of the pile's characteristics are presented in the Table 2.2. The behavior of the pile is modelled by an elastic isotropic model, where the elasticity modulus and the poisson ratio are 70GPa and 0.3 respectively. In addition, the unit weight of the aluminum is $\gamma=27kN/m^3$, which is one of the parameters that are required by the PLAXIS.

Table 2.2 Model Pile Characteristics

Outer Diameter	Thickness	Inner Diameter	Length	Elasticity Modulus	Moment of Inertia
(m)	*(m)*	*(m)*	*(m)*	*(GPa)*	*(m4)*
1.8	0.1	1.6	24	70	0.194

2.3.3 Soil-Pile Interaction

As already mentioned, the PLAXIS model was developed to be as close as possible to the centrifuge model. Therefore, it is important to create a realistic interface for the soil and the pile. In the Appendix, a picture of the pile is presented. As it could be seen, the strain gauges and the glue that has been placed as a sealing means create a really rough surface in the external of the pile. Therefore, although the ordinary choice is to have an interface with a friction angle δ equal with 2/3 of the eternal friction angle φ, in this certain case it is more valid to choose an interface with an external friction angle equal with the internal friction one, hence δ=φ. On the same context, the analyses that will be performed are loaded with a monotonic push, where the soil resistance is mainly offered by the normal horizontal stresses, in contrast to the shear stresses which are critical for the vertical loading. As a result, the interface is not expected to have a considerable impact in the results.

2.4 Series of Analyses

The PLAXIS analyses can be divided into two categories, the main set of analyses that are presented in the following chapter and the preliminary ones that are presented in the Appendix. The first category includes the investigation of the effect of the vertical load, the scour type and depth and the scour protection layer in the lateral soil capacity and stiffness. The vertical load simulations are identical tests in which the vertical dead load is ranged from 0.0MN to 3.0MN with a step of 0.5MN, including therefore seven simulations. The scour investigation contains parametrical analyses of the scour type (narrow, wide and global) and of the scour depth (0.5D, 1.0D, 1.5D and 2.0D), while the vertical dead load is equal to 3.0MN, that is the typical dead load that a wind turbine transfers to the monopile and hence to the soil. Every possible combination between the scour type and the scour depth is investigated and consequently twelve analyses are carried out for this investigation. The last part of the main set of analyses is the scour protection simulations. In this set, three different tests are carried out, in which the diameter of the scour protection is 3.0D, 5.0D and 7.0D. The rest of the parameters are constant,

with a vertical load of 3.0MN been applied for the same reasons as in the scour formation test. The second category, the preliminary tests contain analyses regarding the incremental filling ratio and the interface properties. It needs to be stated that based on the results of these two parameters, it was decided that in all the simulations of the main set of analyses an IFR of 77.5% will be used and no reduced strength is needed for the interface between pile and soil.

Table 2.3 Series of numerical analyses performed in the PLAXIS

		Vertical Load Set of Analyses		
	Scour Type	***Scour Depth***	***Dead Load(MN)***	***Loading***
1	-	-	0.0	Monotonic Push
2	-	-	0.5	Monotonic Push
3	-	-	1.0	Monotonic Push
4	-	-	1.5	Monotonic Push
5	-	-	2.0	Monotonic Push
6	-	-	2.5	Monotonic Push
7	-	-	3.0	Monotonic Push
		Scour Formation Set of Analyses		
	Scour Type	***Scour Depth***	***Dead Load(MN)***	***Loading***
1	Narrow	0.5D	3.0	Monotonic Push
2	Narrow	1.0D	3.0	Monotonic Push
3	Narrow	1.5D	3.0	Monotonic Push
4	Narrow	2.0D	3.0	Monotonic Push
5	Wide	0.5D	3.0	Monotonic Push
6	Wide	1.0D	3.0	Monotonic Push
7	Wide	1.5D	3.0	Monotonic Push
8	Wide	2.0D	3.0	Monotonic Push
9	Global	0.5D	3.0	Monotonic Push
10	Global	1.0D	3.0	Monotonic Push
11	Global	1.5D	3.0	Monotonic Push
12	Global	2.0D	3.0	Monotonic Push
		Scour Protection Set of Analyses		
	Scour Protection Length (D)		***Dead Load(MN)***	***Loading***
1	3.0		3.0	Monotonic Push
2	5.0		3.0	Monotonic Push
3	7.0		3.0	Monotonic Push
		Preliminary Set of Analyses		
	IFR	***Interface Friction***	***Dead Load(MN)***	***Loading***
	77.5%	δ=φ	3.0	Monotonic Push
	77.5%	δ=2/3φ	3.0	Monotonic Push
	50%	δ=φ	3.0	Monotonic Push
	20%	δ=φ	3.0	Monotonic Push

Chapter 3

Results & Discussion

In this chapter, the results of all the series of the numerical analyses are presented and then discussed. For a better overview, the contents of this chapter are divided into five subchapters, dealing with the effect of a certain parameter each time in the lateral soil capacity, while the last part contains design recommendations based on the outcome of this report.

In Figure 3.1 the convention of the failure condition of an offshore pile is presented. More specifically, the system of the soil and pile is considered to have failed when the horizontal displacement at the soil surface level is equal to 0.1D, where D is the diameter of the pile. Of course, this is only a convention, as the ultimate lateral soil capacity based on the soil properties is generally way larger. However, at the aforementioned displacement of 0.1D, the structure is getting quite unstable, considering also the constant cyclic loading in real case conditions, not allowing the safe functionality of the wind turbine. Therefore, from now on, in all the cases below the term failure corresponds to a surface displacement of 0.1D. It needs to be stated that in cases of scour formation or protection in which the soil surface is changed, the displacement of 1.0D is still measured to the original surface level, as depicted in Figure 3.1. On the same context, the reference surface for the depth in every case is the original surface.

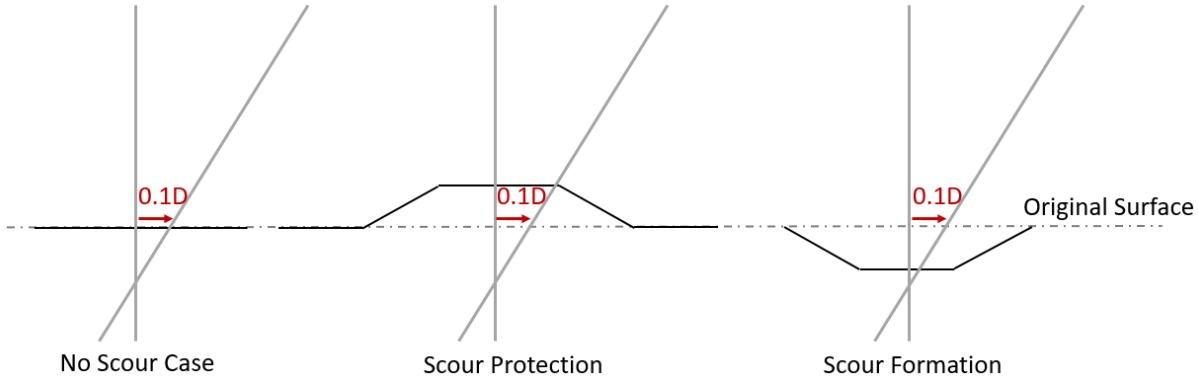

Figure 3.1 Soil surface displacement at which failure of the soil-pile system is considered to occur.

3.1 Vertical Load Effect on Lateral Capacity

In Figure 3.2 the effect of the vertical load in the lateral capacity is presented. More specifically, the load-displacements curves for seven different dead loads, from 0.0MN to 3.0MN at a step of 0.5MN are depicted. It can be seen that the increase of the vertical load has a positive influence in the vertical lateral capacity of the soil-pile system. However, this increase cannot be characterized as crucial since for every 0.5MN higher vertical load, the lateral capacity of the pile in the failure state is only about 2.5% larger. In addition, the influence of the vertical load is continuously decreasing from the dead load of 0.0MN to the one of 3.0MN (Table 3.1). Therefore, the vertical load effect in the lateral capacity seems to be negligible in the case of sandy soils with a high initial relative density. It needs to be stated though that even in the case of the dead load of 3.0MN, which is a typical load from a wind turbine, the load is way lower than the ultimate vertical capacity of the monopile. Therefore, the conclusion drawn should be limited for the relatively small vertical loads.

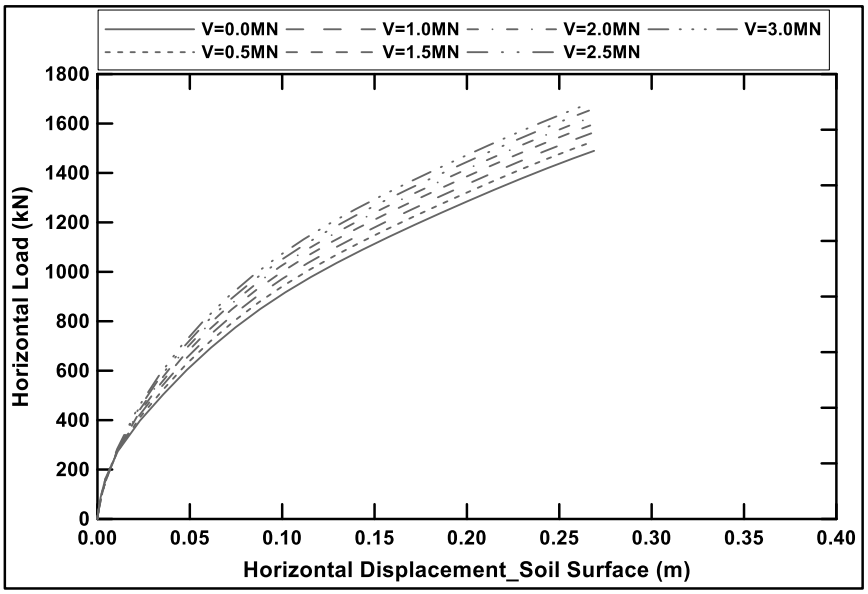

Figure 3.2 Load-Displacement curves for three different dead loads, 0.0MN, 1.5MN and 3.0MN.

In Table 3.1, the lateral capacity for each dead load is presented, along with the increase of the lateral capacity for consecutive vertical loads. It needs to be stated that the clayey soils present quite an opposite behavior, as the increase of the vertical load has a significantly negative influence on the lateral capacity. Therefore, in real case conditions, where the pile is embedded in both in sandy and clayey soil layers, the pile response cannot be predicted based on these simulations.

Table 3.1 Effect of the vertical load of the monopile in the lateral soil-pile capacity.

Failure Load at a Displacement of 0.1D		
Vertical Load (MN)	*Lateral Soil Capacity (kN)*	*Increase Of lateral Capacity (%)*
0.00	1218.16	-
-	-	2.82%
0.50	1253.53	-
-	-	2.56%
1.00	1286.47	-
-	-	2.38%
1.50	1317.87	-
-	-	2.17%
2.00	1347.06	-
-	-	2.09%
2.50	1375.79	-
-	-	1.93%
3.00	1402.93	-

3.2 Effect of the Scour Depth on Lateral Capacity

In Figure 3.3 the load-displacement curves are presented for all the scour simulations. The results are presented in a way that the effect of the scour depth in the lateral capacity can be observed. Therefore, each graph contains the same scour type and all the four different scour depths that have already been mentioned. As it is quite obvious, the increase of the scour depth has a negative influence in the soil lateral capacity, regardless of the scour type that has been formed. This is attributed mainly to the fact that the embedded part of the pile is getting smaller, as the scour depth increases, and therefore, less soil resistance can be mobilized. It is interesting to state that the reduction in lateral capacity as the

scour increases, is obvious even for very small displacements. However, if we examine this reduction in a constant displacement, as the conventional failure one for instance, it seems that the increase of the scour depth will not necessarily decrease proportionally the lateral capacity. Therefore, quantifying this reduction may lead to considerable conclusions. For this reason, Table 3.2 has been conducted.

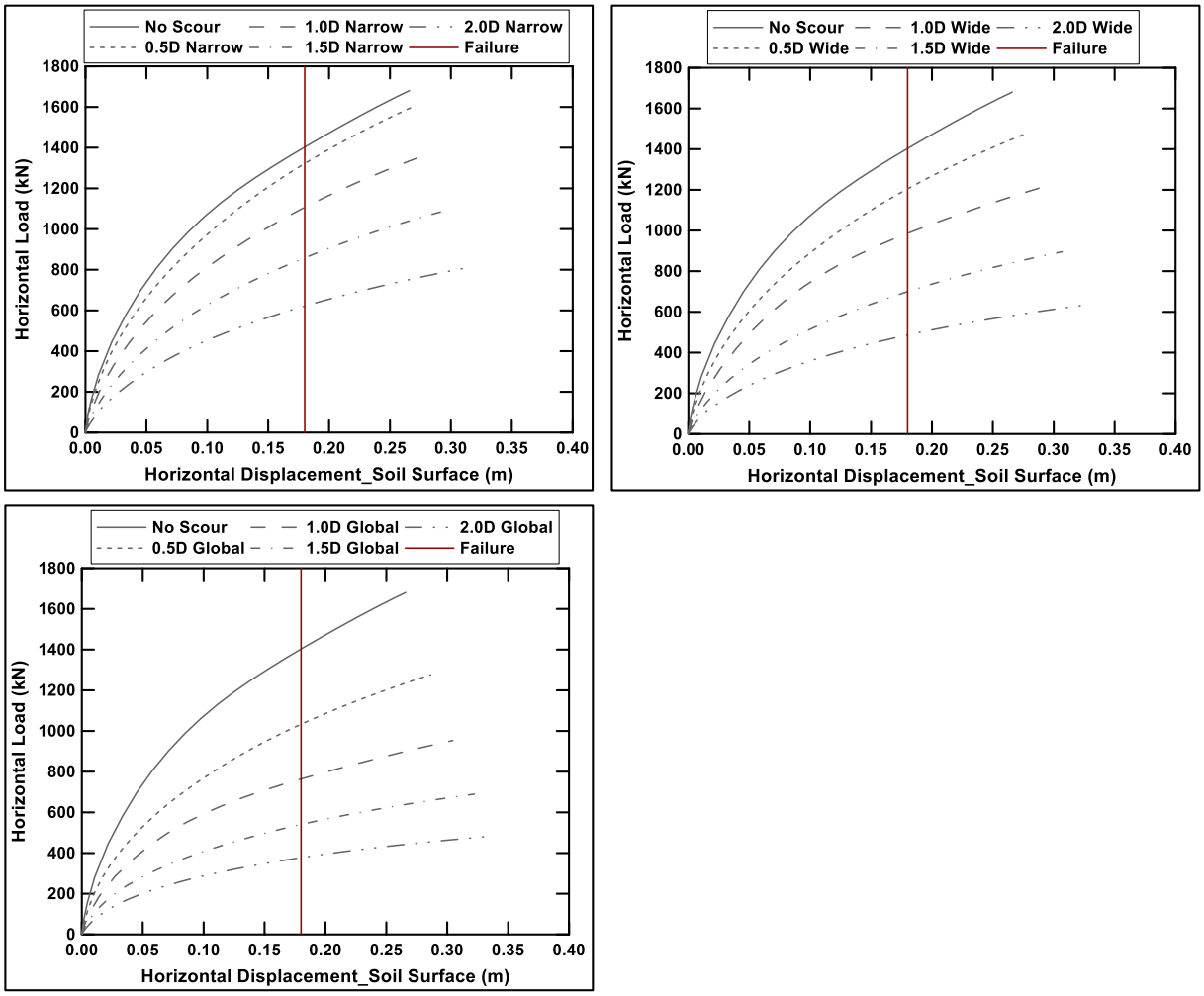

Figure 3.3 Load-Displacement curves for four different scour depths for each of the types of scouring.

As it can be seen in Table 3.2, the scour depth considerably decreases the lateral soil capacity, regardless of the scour type. The case of scour depth equal to 2.0D seems to be non-reversible as in best case scenario, only 40% of the initial capacity remains, while a scour depth up to 1.0D can be manageable, especially in local scour conditions. The table below is presented again in the following subchapter, filled also with the effect of the scour type in the lateral capacity, where a more thorough discussion is made.

Table 3.2 Lateral Capacity at Failure Displacement of 0.1D (kN) for all scour depths.

Lateral Capacity at Failure Displacement of 0.1D (kN)				
No Scour	*Narrow*	*Wide*	*Global*	
1402.927	1322.036	1204.711	1033.301	***0.5D***
	16.29%	*18.17%*	*26.05%*	
	1106.669	985.7842	764.163	***1.0D***
	22.41%	*29.03%*	*29.24%*	
	858.6145	699.6035	540.6947	***1.5D***
	27.58%	*30.48%*	*30.17%*	
	621.8	486.3348	377.5817	***2.0D***

3.3 Effect of the Scour Type on Lateral Capacity

In Figure 3.4 the load-displacement curves are presented for all the scour simulations. The results are presented in a way that the effect of the scour type in the lateral capacity can be observed. Therefore, each graph contains a constant scour depth and the three different scour types that have already been presented.

The same trend is observed in all the four graphs for each scour depth. More specifically, the narrow scour type is the most favorable in terms of lateral soil capacity, while the global scour type is the most critical case. The wide type of scour is an intermediate state, and depends on the length of the horizontal part of the erosion around the pile to define whether it responses closer to the narrow or the global scour type. In our case though, in which this horizontal part is one time the diameter, the behavior of the wide type tends to be much closer to the narrow scour for 0.5D and 1.0D scour depth. On the other hand, in the larger depths, the wide type's response is exactly in the middle between narrow and global type. Therefore, it is clear that the scour formation is a complicated phenomenon, for which the knowledge of either the depth or the type alone cannot give us enough information for a safe prediction of the behavior of the monopile. On the contrary, the combination of scour depth and type dictates the final response of the soil-pile system.

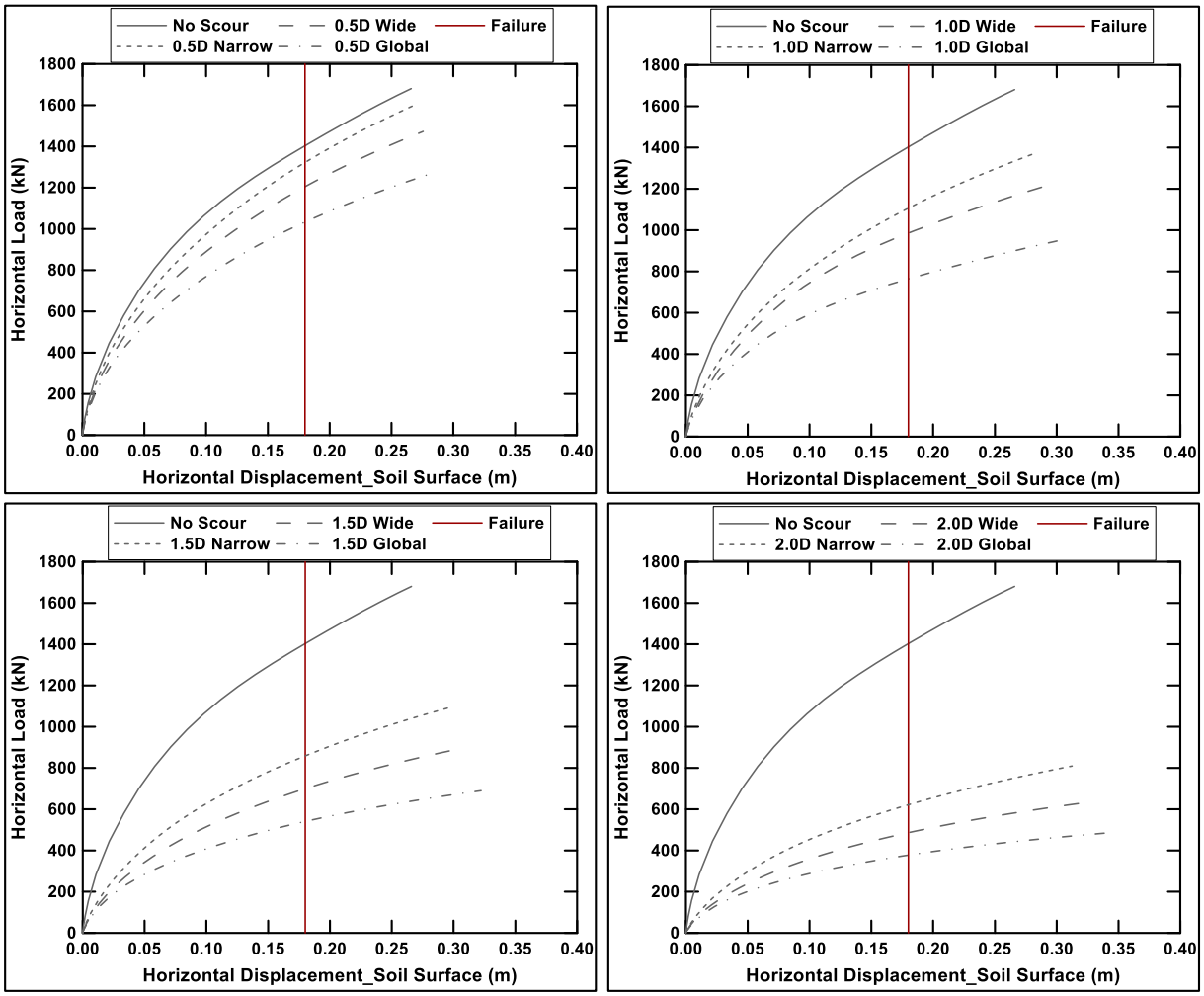

Figure 3.4 Load-Displacement curves for all three different scouring types for each of the scour depths.

To acquire a better understanding of the effect of the scour type in the monopile behavior, the pile deflection and the lateral soil over pressures across its length during the monotonic push are presented in the following graphs (Figure 3.5 & 3.6). More specifically, the pile deflection and the soil pressures have been calculated from 0.0m to 1.0m lateral displacement at the top of the pile with a step of 0.1m.

The failure occurs before the horizontal displacement of 1.0m, but it was considered valid to present the curves even after the conventional failure to better observe the soil behavior. The scour depth of 1.5D has been chosen, as a critical one, since it is a large value, but in the realistic range of the scour depths that have been reported in real case structures.

Figure 3.5 indicates that the pile presents a rigid response in the loading, as it rotates from a point at a depth of about 7m, without any considerable deformation in its axis. It is interesting though to observe that the depth of the rotation point increases from the no scour case, to the narrow, the wide and then to the global type, which is exactly the same sequence as with the lateral soil capacity at the failure displacement. This means that as the soil resistance is reduced due to the soil erosion and the smaller confining pressures, the rotation point is moving downwards in order that equilibrium can be reached in the monopile.

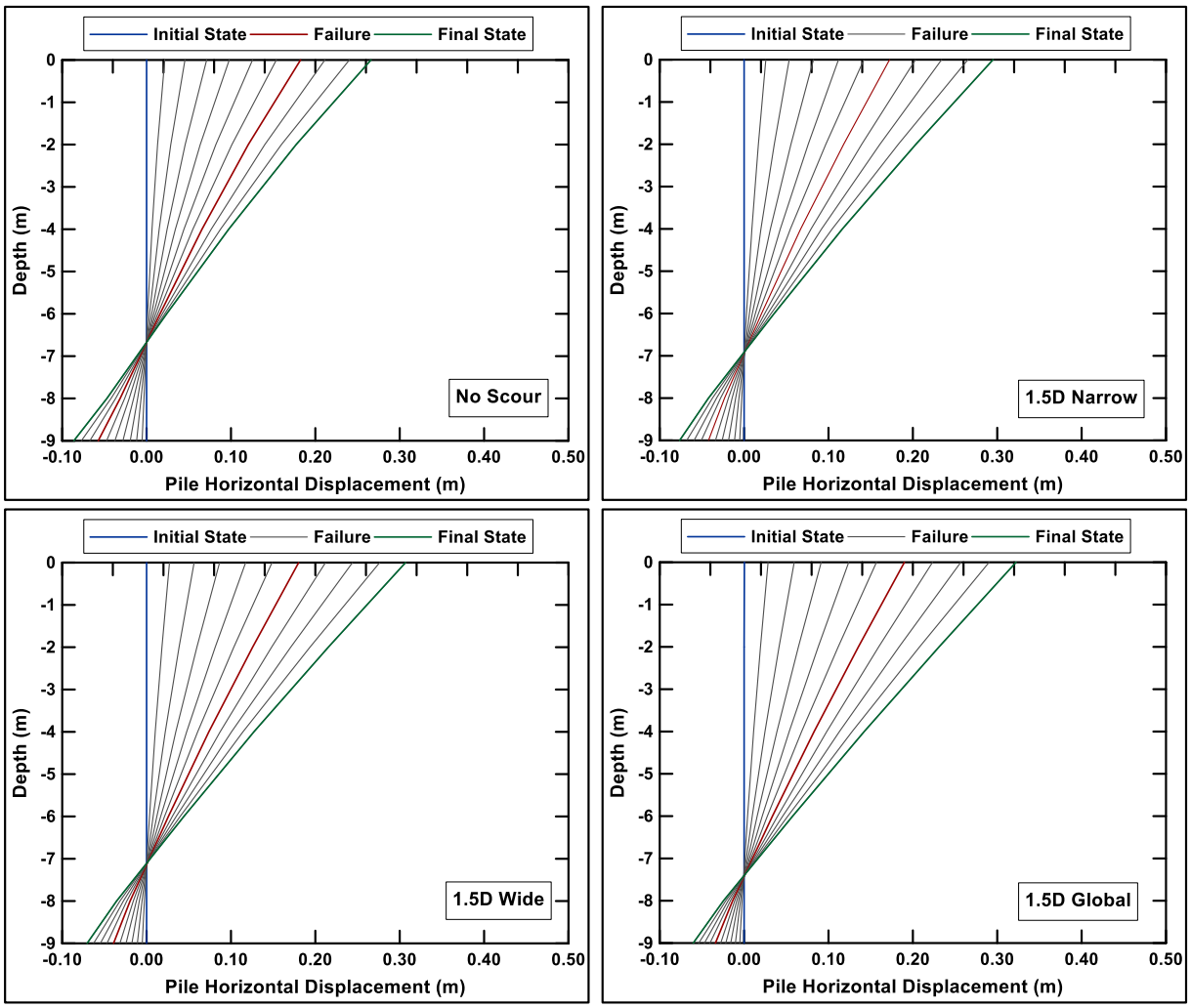

Figure 3.5 Evolution of pile deflection during the monotonic push for the no-scour case and all three scour types for a scour depth of 1.5D.

To further analyze this point, the evolution of the horizontal soil overpressures during the monotonic push can be observed, in Figure 3.6. Despite the fact that the scour depth is constant in all cases, the distribution of the soil pressures is quite different, which is the outcome of the different overburden pressures in the three scour type cases. More specifically, in the narrow type, only a small area of soil is eroded, which means that the reduction in the lateral capacity is mainly caused by the smaller embedded length. On the global scour case though, the much smaller lateral capacity is result of two factors, the smaller embedded length as before, and the significantly lower overburden pressures around the monopile, as the soil has eroded in a vast area. Therefore, the confining pressures around the

monopile are considerably smaller, leading to a lower ultimate soil capacity. This conclusion can be confirmed by the fact that in the narrow case graph, the maximum pressure in the upward part of the pile is located at a depth of 4m with a value of about 800kPa, while in the global scour case the equivalent maximum pressure is only 600kPa in a depth of 5m. This is attributed to the fact that in the global case there is not enough soil resistance in the shallow depths, due to the small overburden pressure and consequently, more soil resistance has to be mobilized in larger depths.

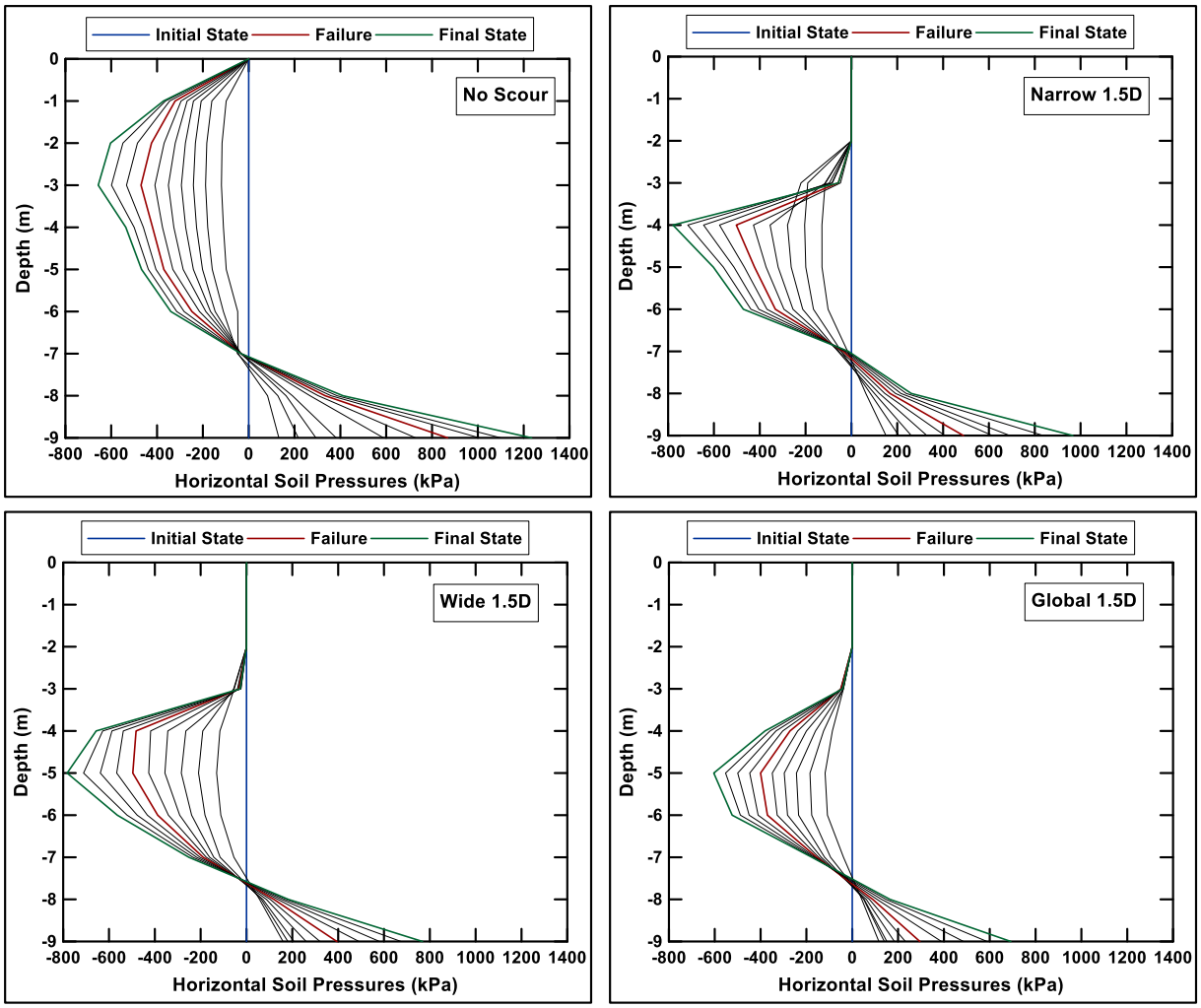

Figure 3.6 Evolution of horizontal soil overpressures during the monotonic push for the no-scour case and all three scour types for a scour depth of 1.5D.

A characteristic part in all the graphs in Figure 3.6 is the "toe-kick" at the depth of 9m, which is a typical behavior of a rigid pile, which makes it quite different from a slender pile. This small detail however, is really important, as it can explain partly the failure of the API method to fully capture the behavior of the offshore piles, as the API regulations have been derived for long and slender piles. However, the rigidity of the offshore piles is crucial and defines their behavior determinately, as the evolution of the soil pressures is affected by it. The same trends are in general common in all depths and scour types and therefore, have not been presented again, as they lead to the same conclusions. The scour analyses results are briefly presented in Table 3.3, to quantify the scour effect, both of the type and the depth.

More specifically, the lateral capacity of the soil-monopile system at failure displacement of 0.1D for all scour depths and scouring types is presented, along with its reduction between consecutive values. It is interesting to observe that both the depth and type of scour can lead to no-return situations. More specifically, the global scour type at all depths, except from the 0.5D, seems to lead to irreversible state, as the capacity is reduced significantly, around 50% at the best case scenario. On the same context,

the scour depth of 2.0D seems to have the same effect on the monopile, as regardless the scour type that is developed, the maximum capacity is about 40% of the original one. Of course, the worst combination of global scour type with a soil erosion of 2.0D literally vanish the original capacity as it is less than 30% of it. The most interesting observation is the impact of the scour type, as obviously anyone would expect the radical drop in the capacity due to the erosion of the soil and the decrease of the embedded pile length. Consequently, during design both scour depth and type should be equally examined to avoid possible undesired situations. In general, it could be concluded that up to 1.0D scour depth the reduction of the lateral capacity may be managed, possibly apart from the global case. However, if the scour depth increases, then the monopile response in lateral loading becomes more critical and it can be managed only for certain types of scour, which the narrow type and in certain conditions the wide type. Of course, if the scour hole becomes too deep, more than 2.0D, even in the narrow scour case, the loss in the capacity is too great, leading to a no-return situation. Last but not least, the analyses conducted for the 0.5D indicate that this scour depth is too small to really affect the problem in narrow and wide type, while in the global type its impact is larger but still completely under control.

Table 3.3 Lateral Capacity at Failure Displacement of 0.1D (kN) for all scour depths and scouring types.

Lateral Capacity at Failure Displacement of 0.1D (kN)						
No Scour	*Narrow*		*Wide*		*Global*	
1402.927	1322.036	*8.87%*	1204.711	*14.23%*	1033.301	***0.5D***
	16.29%		*18.17%*		*26.05%*	
	1106.669	*10.92%*	985.7842	*22.48%*	764.163	***1.0D***
	22.41%		*29.03%*		*29.24%*	
	858.6145	*18.52%*	699.6035	*22.71%*	540.6947	***1.5D***
	27.58%		*30.48%*		*30.17%*	
	621.8	*21.79%*	486.3348	*22.36%*	377.5817	***2.0D***

3.4 Effect of the Scour Protection on Lateral Capacity

In Figure 3.7 the load-displacement curves are presented for the three scour protection simulations that have been performed. In all three cases the surface load is constant at 15kPa, while the diameter of the protection is ranged from 3.0D to 7.0D with a step of 2.0D.

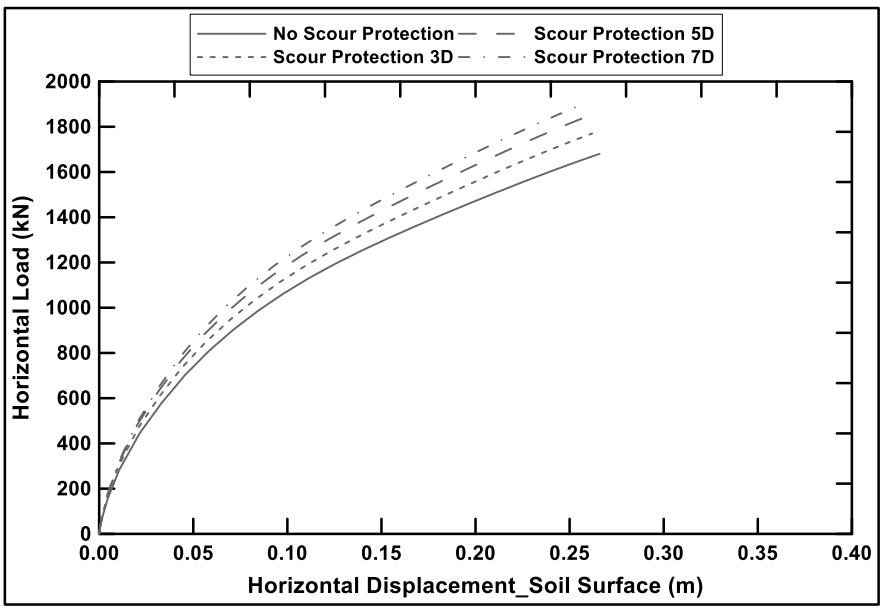

Figure 3.7 Load-Displacement curves for no protection and all three scour protection's diameters.

As expected, the scour protection has a positive influence in the lateral soil capacity. This can be attributed to the increase of the overburden soil pressure, in the same way as the narrow scour case is more favorable than the global scour case for the same depth. In Table 3.3 the lateral soil capacity in the conventional failure displacement is presented for the no protection and the three protection cases in order to quantify the aforementioned positive influence. As it can be seen, the lateral capacity is getting slightly larger with an increase of about 5% for the 3.0D case and around 12% for the best case scenario. Therefore, it can be concluded that the contribution offered is not really large, and therefore it could be ignored during the design phase. However, in cases in which the scour protection layer is larger, the increase in the lateral capacity could be large enough to be taken into account, leading to a more economical design by reducing the required embedded pile length.

Table 3.3 Effect of the vertical load of the monopile in the lateral soil-pile capacity.

Failure Load at a Displacement of 0.1D		
Scour Protection Length (D)	*Lateral Soil Capacity (kN)*	*Increase Of lateral Capacity (%)*
0.0	1402.93	-
-	-	5.41%
3.0	1483.13	-
-	-	4.44%
5.0	1551.99	-
-	-	3.25%
7.0	1604.11	-

Figure 3.8 presents the evolution of the pile deflection during the monotonic push from 0.0 to 1.0m with a step of 0.1m for the no protection case and the scour protection 5D. It can be observed that the displacements are slightly smaller in the scour protection graph, but in general the response is almost the same, as it was also seen in the load-displacements curves. Therefore, the scour protection does not seem to offer a considerable extra lateral capacity of the soil-monopile system.

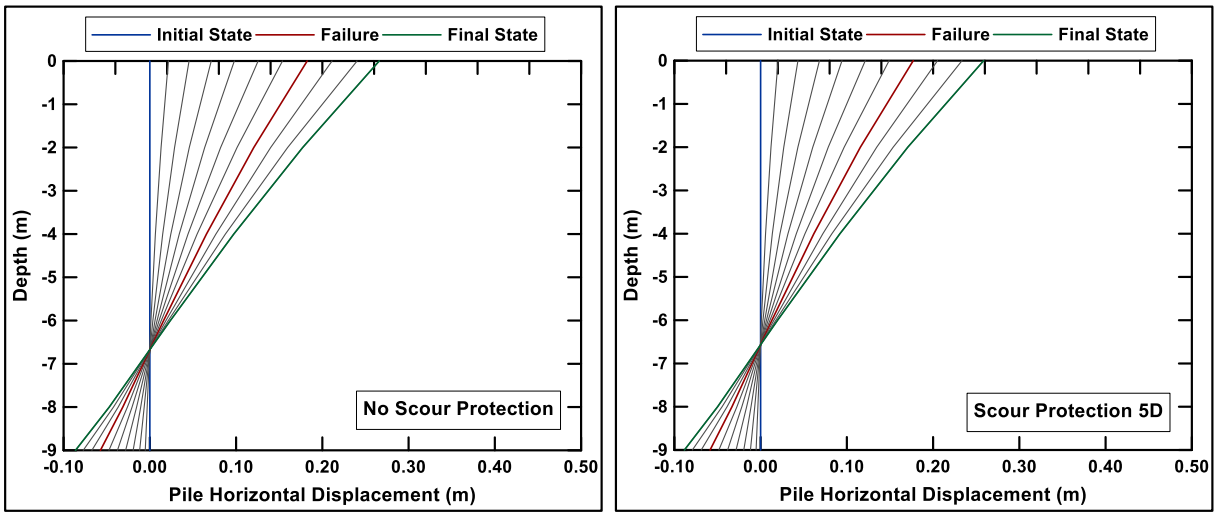

Figure 3.8 Evolution of pile deflection during the monotonic push for the no-protection case and the scour protection of a diameter of 5D.

The slight increase in the lateral soil capacity as the scour protection is installed can be explained by the graph 3.9, in which the evolution of the horizontal overpressures across the length of the pile are presented during the monotonic push from 0.0 to 1.0m with a step of 0.1m for the no protection case and the scour protection 5D. More specifically, it is clear that in the first two meters more soil resistance is mobilized after the scour protection layer. This is attributed of course to the higher overburden pressures due to the protection layer that increase the confining pressures of the soil around the pile

and hence its strength. In the deeper part though, there are only negligible differences between the two curves, which indicates that the load-displacement curves of the two cases differ with each other only due to the soil response in the first two meters.

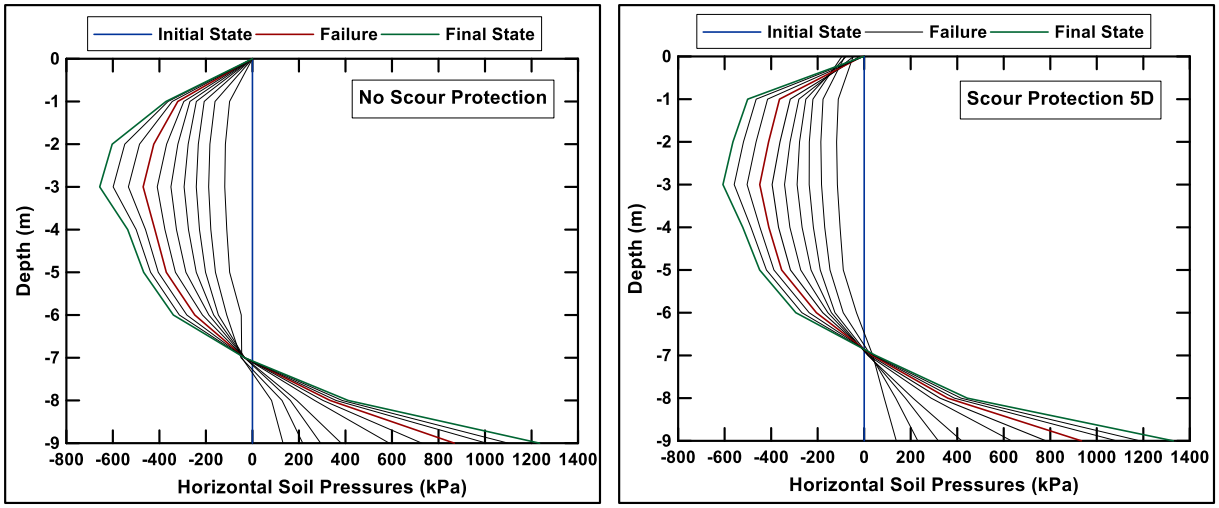

Figure 3.9 Evolution of horizontal soil overpressures during the monotonic push for the no-protection case and the scour protection of a diameter of 5D.

3.5 Design Recommendations for Scour Formation

As it was analytically described in the first chapter, the API method has been rendered as an outdated method for describing the rigid monopiles' response. Therefore, using this method for quantifying the effect of the scour formation in the soil-monopile stiffness and lateral capacity is not considered to be valid. For this reason, it was decided to measure the scour effect in the lateral soil capacity and in the soil stiffness when the displacement of the pile in the soil surface reaches the failure displacement of 0.1D, as it is established in the literature. More specifically, the aim of this chapter is to produce normalized graphs that will correlate the lateral capacity and stiffness of the no scour case with both the scour depth and type. Then, the aforementioned charts could be used in the design of rigid offshore monopiles in sandy soils. Obviously, the final designing process cannot be based on charts, as every case is sensitive to the local soil conditions and detailed numerical analyses are required. However, the initial stages, the feasibility ones, require fast calculations based on scientific background though, and therefore the graphs produced can be applied. On the same context, the verification of numerical analyses can also be performed though the output of research conducted in the same area.

The first chart (Figure 3.10) correlates the horizontal load at 0.1D displacement of the pile in the soil surface with the scour depth and the scour of the type. The load is normalized by being divided with the unit weight and the diameter to the power of three, and the scour depth is divided by the pile diameter as well. Obviously, all the curves start from the same point, as for zero scour depth, they all correspond to the no scour case. It is interesting to observe that the difference in the horizontal load for the three curves is larger from 1.00 to 1.50 and getting smaller as it reaches the 2.0D scour depth, where the curves converge. This indicates that the scour type is critical in a certain range of depths, but after a certain limit it does not really affect the problem as the erosion of the soil is too extreme. Getting in a depth larger than 2.0D is pointless as in the literature such a value never reported, which of course makes sense, as the pile would have collapsed in such an extreme erosion. It is also interesting to observe that the narrow type curve is more a concave one, while the wide type (after the 0.5D) and the global type curves are more like to convex ones. That clearly points out the fact that the narrow scouring type becomes critical after the 1.5D, as its lateral capacity is slowly reducing before that point. On the other hand, the global type, which is displayed by the convex curve, loses its initial resistance quite fast, proving that it can be critical even in relatively small scour depths.

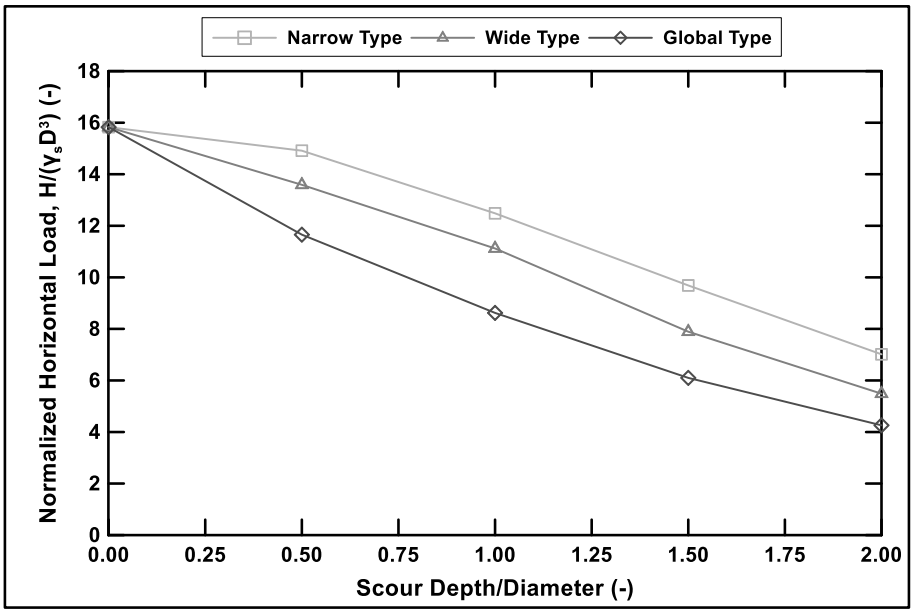

Figure 3.10 Horizontal Load versus scour depth for the three different scouring types at a failure deformation of 0.1D at the original soil surface.

The second chart (Figure 3.11) that has been produced correlates the soil stiffness at 0.1D displacement of the pile in the soil surface with the scour depth and the scour of the type. The stiffness is normalized by dividing the load with the unit weight, the embedded pile length and the diameter to the power of two, and the scour depth is divided by the pile diameter similarly to Figure 3.10.

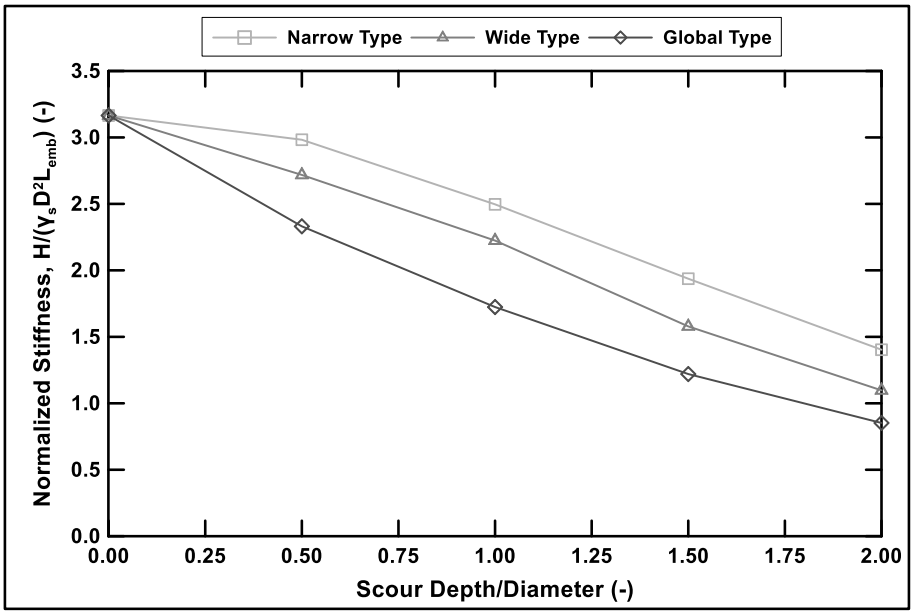

Figure 3.11 Stiffness versus scour depth for the three different scouring types at a failure deformation of 0.1D at the original soil surface.

The trends in the evolution of stiffness with respect to the scour depth and type are the same ones that have been observed in the previous graph, as they both have occurred by the horizontal load. However, it is interesting to extract the results both for the normalized horizontal load and the normalized stiffness as they can both be applied during the design phase. Therefore, for a better overview of the results it was chosen to present both Figure 3.10 and 3.11.

Chapter 4

Conclusions

In this current project, the effect of the scour formation (both with respect to depth and type) on the stiffness and the lateral capacity of a rigid monopile in offshore conditions under monotonic push was investigated. The methodology followed for conducting this research included 26 numerical analyses in the finite element code of PLAXIS 3D, all in sand. The main findings that have been extracted by all the aforementioned tests and analyses are discussed below and evaluated.

Firstly, it was decided to investigate the impact of the vertical load in the lateral soil capacity in a typical monopile. It was shown that the increase in the vertical load has a positive influence in the lateral capacity of the soil-monopile system. However, this increase in the soil resistance when measured in a pile displacement of 0.1D at the soil surface, that is considered to be a failure point, was about 5%. Therefore, it could be characterized negligible, which is in accordance with the literature that indicates that in sandy soils the vertical load has no effect or slightly positive in lateral loading, in contrast to the clayey soils where the opposite behavior occurs.

In the main content of results, the first conclusion drawn are about the scour depth impact on the stiffness and lateral capacity of the soil. More specifically, it was shown that for the same type of scouring, the increase of the depth of the scour hole can significantly reduce the soil resistance, as expected. It is interesting though to note, that in general scour up to 1.0D is manageable except for the global scour case possibly. However, as the scour depth increases, the situation becomes more critical and in depth of about 2.0D, the loss of the capacity is so great that a no-return state is expected, regardless of the scouring type. The mechanism that determines this soil's capacity reduction is based on the shortening of the embedded pile length. More specifically, in order to compensate the erosion of the soil in the upper layers, more soil resistance is mobilized in the lower soil layers that the pile is installed on. However, as the embedded length is decreasing, the mobilized resistance may be exhausted in the whole length, as the soil will reach the plastic zone and then the critical state behavior. Therefore, it is clearly indicated that scour formation's depth is critical, and during design it needs to be taken into account, to consider up to which depth the soil erosion can be dealt with.

The next scour parameter that was investigated was the type of scouring, as local scour (narrow and wide) or global can occur. It was shown that this term had a great impact on the lateral soil capacity. More specifically, the narrow type of scour was the most favorable case, which could approach the no scour case for small scour depth, while the global scour case was the most critical, as even in small scour depths could lead to dramatic reduction of the capacity. The main point is that the narrow case and the wide one can be manageable in depths up to 1.5D under certain conditions, while the global type seems to become a no-return case for much smaller erosion depths. The effect of the scour type in the soil capacity and stiffness is attributed to the change in the overburden pressure that occurs after the soil erosion. More specifically, as the soil is washed away, the overburden pressure is reduced in the soil being in the sides of the pile. This reduction is getting too extreme in the global scour case, leading to undesired effects, while in the narrow case a relatively small volume of soil is eroded and may be critical only if combined with deep scour hole. Obviously, the wide type is between the two other that can act the lower and upper limit of the scour type effect in the lateral soil capacity.

After the scour formation, the scour protection investigation was followed. More specifically, three analyses have been conducted with different protection layer's diameters, 3.0D, 5.0D and 7.0D. Despite the clear increase of the lateral capacity in the conventional failure displacement at 0.1D, the contribution of the protection layer was not more than 15% in best case scenario, as it ranged from 5% to 15%. Therefore, it could be neglected in the design phase, though for thicker protection layers comparing to the typical 1.0m that was used in the analyses, its contribution could be taken into account and reduce the required embedded pile length.

The soil pressures and the pile deflections that have been extracted by the numerical investigation clearly point out that the monopile presents a rigid response. More specifically, the pile was rotated in all cases from a rotation point, presenting a toe kick behavior as high soil pressure were developed in the downward part of the pile, with different direction of the ones in the upper part. This rigid behavior of the pile clearly indicates that the API method is outdated as it is based on slender piles and in no way can capture the toe kick and the rotation point, which are crucial in defining the soil pressures. Since the p-y curves by the API method are not suitable for the aforementioned piles, it was considered valid to recommend a design chart based on the analyses conducted that will correlate the stiffness and the lateral load of the monopile at failure with the scour depth and type. This chart decided to be normalized and used for assessing the impact of the scour formation in soil resistance in offshore monopile problems.

References

Achmus, M., Kuo, Y.-S., & Abdel-Rahman, K. (2009). Behavior of monopile foundations under cyclic lateral load TT. Computers and Geotechnics TA, 36(5), 725–735.

API (American Petroleum Institute) (2011). Geotechnical and foundation design considerations, ANSI/API recommended practice 2 GEO, 1st edn. Washington, DC, USA: API

Atkinson, J. H., Richardson, D., & Stallebrass, S. E. (1990). Effect of recent stress history on the stiffness of overconsolidated soil. Géotechnique, 40(4), 531–540.

Azua Gonzalez, C. (2017). Dynamic Finite Element Analysis of Impact Pile Driving Centrifuge Tests. TU Delft.

Bauer, E. (1996). Calibration of a Comprehensive Hypoplastic Model for Granular Materials. Soils and Foundations, 36(1), 13–26.

D. Mašin, Calibration of sand hypoplastic model on Geba sand data, Internal report issued for
de Jager, R. R., Maghsoudloo, A., Askarinejad, A., & Molenkamp, F. (2017). Preliminary Results of Instrumented Laboratory Flow Slides. Procedia Engineering, 175, 212–219.

Det Norske Veritas. Design of Offshore Wind Turbine Structures. Technical Report, DNV; 2014. DNV-OS-J101.

Doherty, P., & Gavin, K. (2012). Laterally loaded monopile design for offshore wind farms. Proceedings of the Institution of Civil Engineers - Energy, 165(1), 7–17.

Garnier, J., Gaudin, C., Springman, S. M., Culligan, P. J., Goodings, D., Konig, D., Thorel, L. (2007). Catalogue of scaling laws and similitude questions in geotechnical centrifuge modelling. International Journal of Physical Modelling in Geotechnics, 7(3), 1–23.

Germanischer Lloyd. Guideline for the Certification of Offshore Wind Turbines; 2012, GL.

Hjorth, P. (1975). Studies on the nature of local scour. Lund.

Hoffmans, G. J. C. M., & Verheij, H. J. (1997). Scour manual. Rotterdam, Netherlands; Brookfield, VT: A.A. Balkema.

International Electrotechnical Commission. Wind turbines: Part 3: Design requirements for offshore wind turbines; 2009. IEC61400-3.

Kishore, Y. N., Rao, S. N., & Mani, J. S. (2009). The behavior of laterally loaded piles subjected to scour in marine environment. KSCE Journal of Civil Engineering, 13(6), 403–408.

Kolymbas, D. (1985). A generalized hypoelastic constitutive model. Proc. XI Int. Conf. Soil Mechanics and Foundation Engineering, 5, 2626.

Kuo, Y.-S., & Achmus, M. (2008). Practical Design Considerations of Monopile Foundations with Respect to Scour.

LeBlanc, C., Houlsby, G. T., & Byrne, B. W. (2010). Response of stiff piles in sand to long-term cyclic lateral loading. Geotechnique, 60(2), 79–90.

Lin, C., Bennett, C., Han, J. & Parsons, R. L. (2010). Scour effects on the response of laterally loaded piles considering stress history of sand. Comput. Geotech. 37, No. 7–8, 1008–1014.

Matutano, C., Negro, V., López-Gutiérrez, J.-S., & Esteban, M. D. (2013). Scour prediction and scour protections in offshore wind farms. Renewable Energy, 57(Supplement C), 358–365.

McClelland, B., & Focht, J. A. (1980). Soil modulus for laterally loaded piles. International Journal of Rock Mechanics and Mining Sciences & Geomechanics Abstracts International Journal of Rock Mechanics and Mining Sciences & Geomechanics Abstracts, 17(1), A12.

Mostafa, Y. E. (2012). Effect of Local and Global Scour on Lateral Response of Single Piles in Different Soil Conditions. Engineering, Vol.4(No. 6), 297–306.

Niemunis, A., & Herle, I. (1997). Hypoplastic model for cohesionless soils with elastic strain range. Mechanics of Cohesive-Frictional Materials, 2(4), 279–299.

O'Neill, M. W., & Murchison, J. M. (1983). An evaluation of p-y relationships in sands. [Houston, Tex.]: University of Houston.

Petersen, T. U., Mutlu Sumer, B., Fredsøe, J., Raaijmakers, T. C., & Schouten, J.-J. (2015). Edge scour at scour protections around piles in the marine environment - Laboratory and field investigation. Coastal Engineering, 106, 42–72.

Puzrin, A. M., & Burland, J. B. (1998). Non-linear model of small-strain behaviour of soils. Géotechnique, 48(2), 217–233.

Qi, W. G., Gao, F. P., Randolph, M. F., & Lehane, B. M. (2016). Scour effects on p–y curves for shallowly embedded piles in sand. Géotechnique, 66(8), 648–660.

Reese, L. C., & Matlock, H. (1956). Non-dimensional solutions for laterally-loaded piles with soil modulus assumed proportional to depth. Dallas, Tex.: Association of Drilled Shaft Contractors.

Reese, L. C., Cox, W. R., & Koop, F. D. (1974). Analysis of Laterally Loaded Piles in Sand. Offshore Technology Conference.

Reese, L. C., Wang, S., & Long, J. (1989). Scour from cyclic lateral loading of piles. Offshore Technology Conference. https://doi.org/10.4043/6005-MS

Royal IHC, Netherlands (Charles University in Prague, 2017).

Sørensen, S. P. H., & Ibsen, L. B. (2013). Assessment of foundation design for offshore monopiles unprotected against scour. Ocean Engineering, 63, 17–25.

Sumer, B. M., Fredsøe, J., & Christiansen, N. (1992). Scour Around Vertical Pile in Waves. Journal of Waterway, Port, Coastal, and Ocean Engineering, 118(1), 15–31.

Verdure, L., Garnier, J., & Levacher, D. (2003). Lateral cyclic loading of single piles in sand. International Journal of Physical Modelling in Geotechnics, 3(3), 17–28.

von Wolffersdorff, P.-A. (1996). Hypoplastic relation for granular materials with a predefined limit state surface. Mechanics of Cohesive-Frictional Materials, 1(3), 251–271.

Wang, J., & Qi, C. (2008). P-y curves of piles in saturated degradation sands with residual pore water pressures. In Proceedings of the International Offshore and Polar Engineering Conference (pp. 690–697).

Whitehouse, R. J. S. (1997). Scour at marine structures: a manual for practical applications. Scour at marine structures: a manual for practical applications. Retrieved from

Whitehouse, R. J. S. (2006). Scour at coastal structures. In 3rd Int. Conf. on Scour and Erosion (pp. 52–59). Amsterdam, Curnet, Gouda, Netherlands.

Whitehouse, R. J. S., Harris, J. M., Sutherland, J., & Rees, J. (2011). The nature of scour development and scour protection at offshore windfarm foundations. Marine Pollution Bulletin, 62(1), 73–88.

Yang, K., & Liang, R. (2007). Methods for deriving p-y curves from instrumented lateral load tests. Geotechnical Testing Journal, 30(1), 31–38.

Appendix

A. Centrifuge Tests

A brief description of the centrifuge experiment that the numerical modeling simulates is given in this subchapter. In Appendix Figure 1, the TU Delft centrifuge beam is depicted along with the device that enables to have horizontal displacement. In Appendix Figure 2, the pile is presented, initially in its own and then after been inserted in the sample in the strongbox.

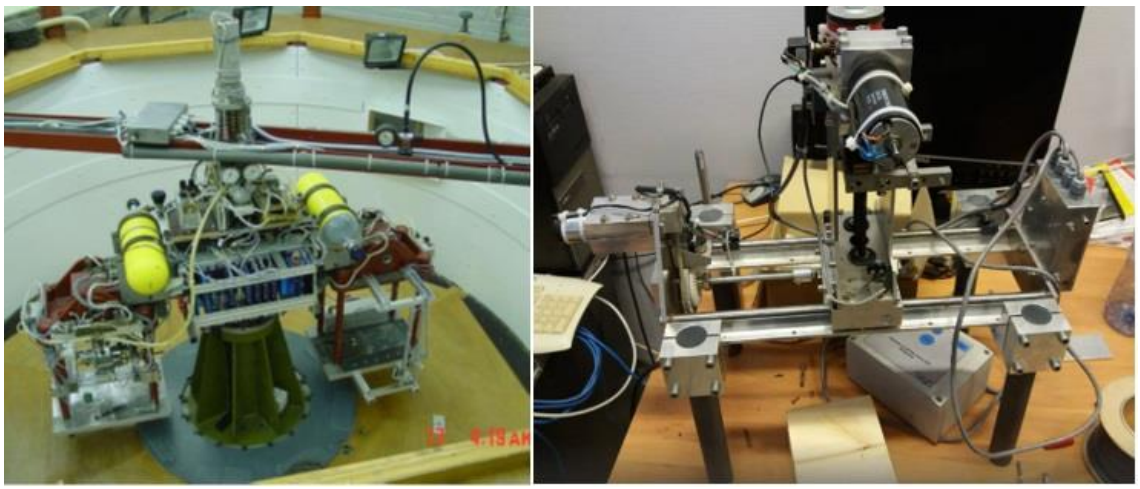

Appendix Figure 1 TU Delft centrifuge beam and actuator for lateral displacement.

Appendix Figure 2 Pile used for the centrifuge experiment in and out the sample.

The sequence that is followed in the centrifuge tests is the following. After the preparation of the sample and its placements in the centrifuge basket, the pile is installed in the sample at 1g. The typical set up

of the experiment is depicted in Appendix Figure 3. After the installation of the pile, the centrifuge room the experiment starts. More specifically, the sample is accelerated up to 100g, and then the monotonic push started with a rate of 0.01mm/s until a horizontal displacement of 3.0mm (equivalent to 3.0m in prototype) was achieved. During the whole duration of the experiment, the load cells' and the strain gauges' measurements are transferred to the main computer, allowing for data implementation afterwards.

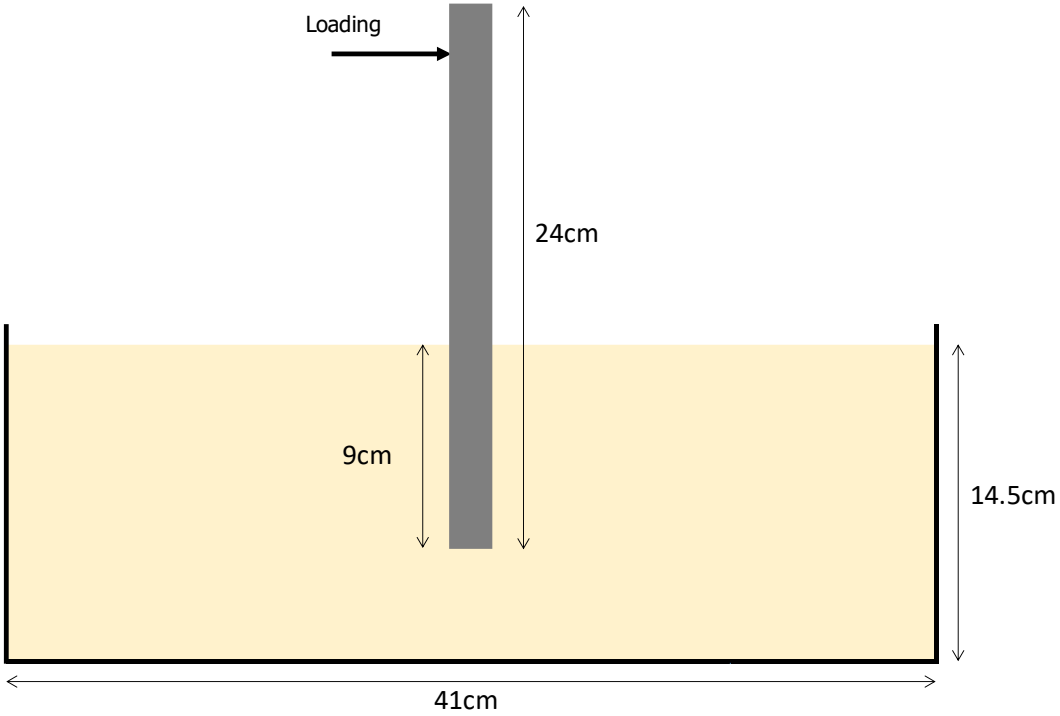

Appendix Figure 3 Typical set up of the centrifuge experiment.

B. IFR & Interface Analyses

In the Appendix Figure 4, the IFR impact on the lateral capacity of the soil is presented. More specifically, three different values of the IFR have been chosen, with the 77.5% and 50% being more realistic and the 20% being an extreme low value.

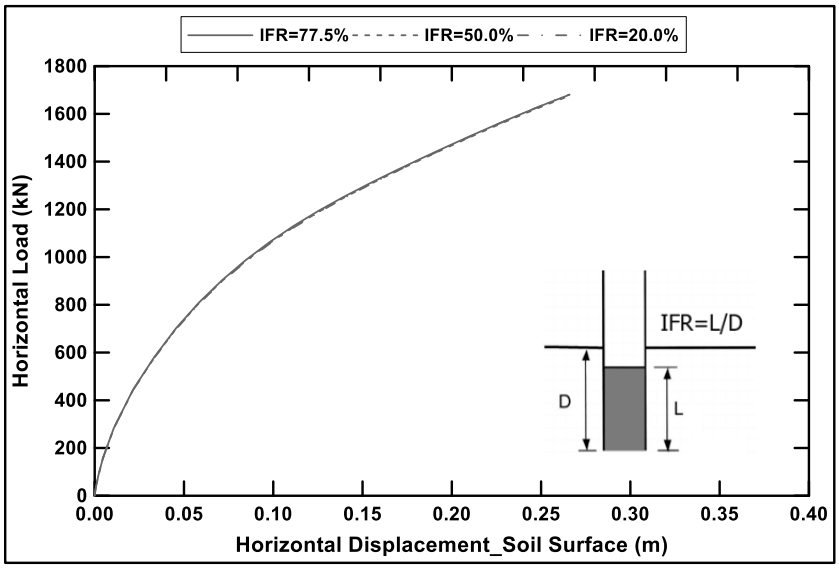

Appendix Figure 4 Load-Displacement curves for different incremental filling ratios.

As it can be seen, the impact of this parameter is not considerable in the lateral capacity of the soil. This can be attributed to the fact that the lateral capacity is mobilized by normal soil stresses, while the shear stresses offer mainly to the vertical capacity to the pile, which is not the case in these analyses. Therefore, it can be concluded that IFR parameter is not going to affect the results and with this in mind, it was chosen to have a pile filled with soil in its interior up to a distance of 1.0D from the new soil surface that occurs for every scour depth. This corresponds to a IFR value of about 77.5% for all cases.

In the Appendix Figure 5, the interface properties' impact on the lateral capacity of the soil is presented. More specifically, two different values of the properties have been chosen, δ=φ and δ=2/3φ. As it was already mentioned, the pile due to the installation of the strains and the glue for water-sealing was really rough in its external surface. On the same context, due to the cables of the strains in the interior of the pile, equally rough internal surface is expected. Therefore, the δ=φ case is considered to be the more realistic value for defining the interface properties. As it can be seen in the graph below, the δ=φ case offers higher soil resistance than the δ=2/3φ case. However, their difference, especially in the area of failure is quite small, less than 5%. Consequently, it was chosen to use the interface with properties δ=φ, as this case was considered more realistic and in any case the influence of this parameter is not at any point critical in the horizontal soil capacity.

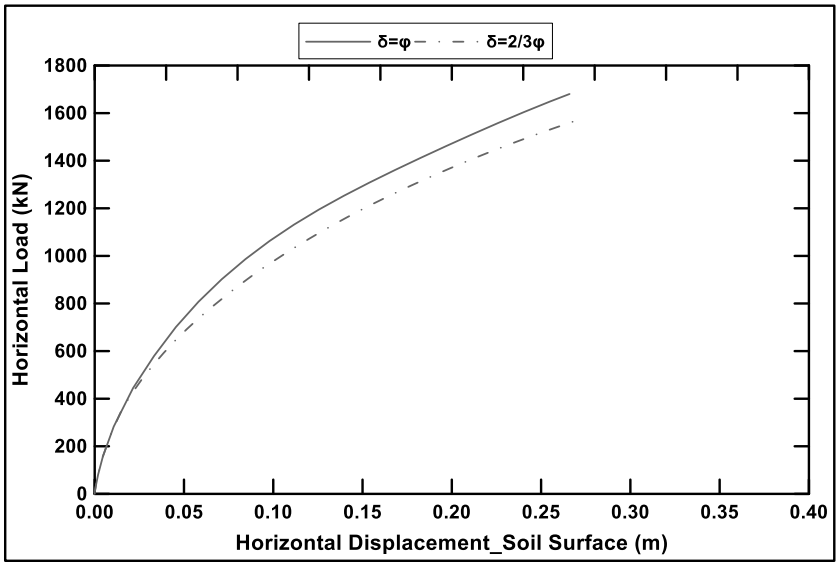

Appendix Figure 5 Load-Displacement curves for different interface properties.